NASA Applied Information Systems Research (AISR) Grant NNX07AL32G
Applied Physics Laboratory Task FG2EC
"INTELLIGENT SENSOR NETWORK STUDY OF DUST DEVILS".
Progress Report April 2008- April 10, 2009
Ralph D. Lorenz, Principal Investigator 4/11/09

In April 2008, an array of 20 Crossbow wireless motes was field-tested. Although individual motes performed satisfactorily (and a dust devil was detected by several nodes of the array), it was found that the message-handling protocol of the wireless network did not sustain adequate throughput to adequately record meteorological parameters from the more distal nodes in the array. Specifically, the nodes at the far corner of the 20-station array with 5m spacing took 5-10 seconds before their values were refreshed, suggesting that scaling up to a larger array would not achieve the desired results.

Efforts since have been devoted to designing a custom datalogger, using USB memory stick to provide essentially unlimited storage, and solar power to provide essentially unlimited energy (the September 2007 trial of PICaxe dataloggers showing that battery replacement for a large array can be very time-consuming). The elements of this logger design (sized to permit an array of 80 units to be brought to the field in a single piece of checked airline luggage) have all been prototyped and the printed circuit board for the logger is being laid out. It is expected that field data will be obtained in the June and/or September field seasons in Arizona. Informal discussions with Steve Metzger of PSI suggest his field site in Boulder Canyon, NV may be suitable in August (when monsoons usually suppress Arizona dust activity) providing other options.

Review of the dust devil literature to refine expectations of the number of devils to be encountered has led to a short paper 'Power Laws of Dust Devils on Earth and Mars', submitted to Nature Geoscience (1).

Field testing of instrumentation was carried out in Death Valley National Park in December 2008/March 2009, with favorable results. A timelapse camera design suitable for documenting the dust devil activity to be monitored with the datalogging array above has been now reached (battery undervoltage issues leading to filesystem corruption on the SD memory cards have been worked around), and successfully operated in the field for 100 days. Experiments with accelerometer-based wind sensing were also conducted and results are being reviewed for possible implementation on the datalogging array.

A paper on the timelapse camera approach has been submitted to Journal of Atmospheric and Oceanic Technology (2), and the results of the field tests on the meteorological conditions in Death Valley has been written up in a paper submitted to Journal of Applied Meteorology and Climatology (3).

Submitted manuscripts (1), (2) and (3) are attached – note that referees comments have not yet been received so the final versions (if any) may differ from the original submissions.

Power Laws of Dust Devils on Earth and Mars

R. D. Lorenz[1]

[1]Johns Hopkins University Applied Physics Laboratory, Laurel, MD 20723.

Submitted 4/8/09 to Nature Geoscience

~900 Words + 2 Figures. 1 Supplemental Table.

Dust devils[1] are dry convective vortices that loft dirt into the air, often a nuisance for outdoor activities and occasionally responsible for structural damage and fatal aircraft accidents[2]. They are also the most prominent dynamic phenomena observed on the surface of Mars, where they influence the climate by acting as the principal mechanism of dust-raising. Atmospheric dust, and its removal by dust devils from solar panels, can also significantly impact the operation of spacecraft on the Martian surface. However, estimates of dust devil frequency, even at terrestrial localities known for their abundance, vary by some four orders of magnitude, making a quantitative hazard assessment difficult. Here I show that new high-quality observations from Mars fit a power law size distribution, that such a power law population can unify the discrepant terrestrial surveys, and, indeed, that the populations on the two planets appear similar.

Visual census data obtained by hot and tedious observations over the last 4 decades (see Supplemental Online Material) all agree, as do air accident statistics, on the seasonal and diurnal variation of dust devil activity, which peaks in early afternoon of summer, when the convective heat flux driving the devils is strongest. However, the overall reported populations in terms of dust devils per unit area per unit time are vastly different (see Supporting Table 1). This is a puzzle : while there is evident spatial variation in dust devil frequency owing to dust availability and vorticity generation by terrain (e.g. local counts vary between 1 and 80 per square mile in one survey[3], with dry river beds having the highest observed density), the surveys are by definition performed in areas known to have frequent dust devils and the populations reflect roughly the same summer clear-sky convective heat flux and so should be similar.

Because of the difficulty of measuring size in real time in the outdoors, visual surveys have tended to estimate dust devil diameters with coarse size categories. However, more quantitative analysis tools can be applied at leisure to digitally-recorded images, such as those obtained from landed spacecraft on Mars. Lengthy observations by the Mars Exploration Rover Spirit recorded some 533 dust devils[4] whose sizes were well-determined in 10m size bins. These data are shown on logarithmic axes in figure 1, and the linear trend is consistent with a power law with an exponent of -2 (except in the smallest size bin, not shown, which is depleted due to the existence of a threshold size of either the phenomenon, its detection, or both, which truncates the distribution.)

An exponential function had been proposed[5] on information-theoretic grounds to fit the coarsely-binned diameter statistics of the terrestrial surveys. However the better-quality Mars data shows that an exponential distribution falls off too at large sizes (i.e. its tail is too small : an exponential fit has a correlation coefficient R^2=0.84, while the power law yields a much better R^2=0.94.) A power law, a common distribution for geophysical phenomena, also suggests a clue by which the discrepant terrestrial data can be reconciled.

The surveys span a wide range of sample area, and although detection thresholds are not reported, it is obvious that small dust devils will be difficult to see at long distance. Thus large area surveys will be less efficient at detecting the small, more abundant features. Simplistically, for a constant density with a -2 power law differential size distribution, the cumulative number density of detections exceeding a fixed angular span threshold will fall off linearly (since the cumulative size distribution for a -2 power law differential distribution has a -1 exponent) with detection range, or with the square root of survey area. Other factors, including the suppression of distant optical contrast by atmospheric scattering, can cause the observed density to fall off more steeply. More particularly, if dust devil height and width are correlated, and the detection threshold relates to the solid angle subtended by the feature, then the

number density of detections will fall off as the square of range, or inversely with survey area. This is in fact what is seen (figure 2) which shows that all the surveys from Earth and Mars follow the same relationship of observed density (devils $km^{-2}day^{-1}$)=50/Area(km^2). For the smallest study area of 0.1km^2, the relevant size threshold (taking into account the angular resolution of the naked eye) will be ~0.5m. Adopting this as a general minimum diameter implies a maximum occurrence rate of ~500 devils $km^{-2}day^{-1}$ at 0.5m and above, with e.g. ~50 devils $km^{-2}day^{-1}$ at a diameter of 5m and above, per the -2 differential power law above. This power law perspective finally permits confident general prediction of dust devil hazards and effects.

For a finite population, a power law must be truncated at small and large sizes. It is impossible to say without better (digital) terrestrial data whether the same detection thresholds apply for surveys on Mars and Earth, and thus whether the same intrinsic minimum size applies on the two worlds (the minimum size may relate to the Obhukov length scale[5]). It is noteworthy, that the Martian and terrestrial surveys fall on the same line, suggesting that the underlying populations may be similar, despite the very different atmospheric densities on Earth and Mars.

Acknowledgement

This work was supported by the NASA Applied Information Systems Research program.

Competing Financial Interest

The author has no competing financial interests.

References

1. Balme, M. and R. Greeley, Dust Devils on Earth and Mars, Reviews of Geophysics, **44,** RG3003, 2006

2. Lorenz, R. D. and M. J. Myers, Dust Devil Hazard to Aviation: A Review of US Air Accident Reports, Journal of Meteorology, **30,** 178-184, 2005.

3. Sinclair, P. C., General Characteristics of Dust Devils, Journal of Applied Meteorology, **8,** 32-45, 1969

4. Greeley, R. et al., Active dust devils in Gusev crater, Mars: Observations from the Mars Exploration Rover Spirit Journal of Geophysical Research, **111,** E12S09 , 2006

5. Kurgansky, M., Steady-State properties and statistical distribution of atmospheric dust devils, Geophysical Research Letters, **33,** L19S06, 2006

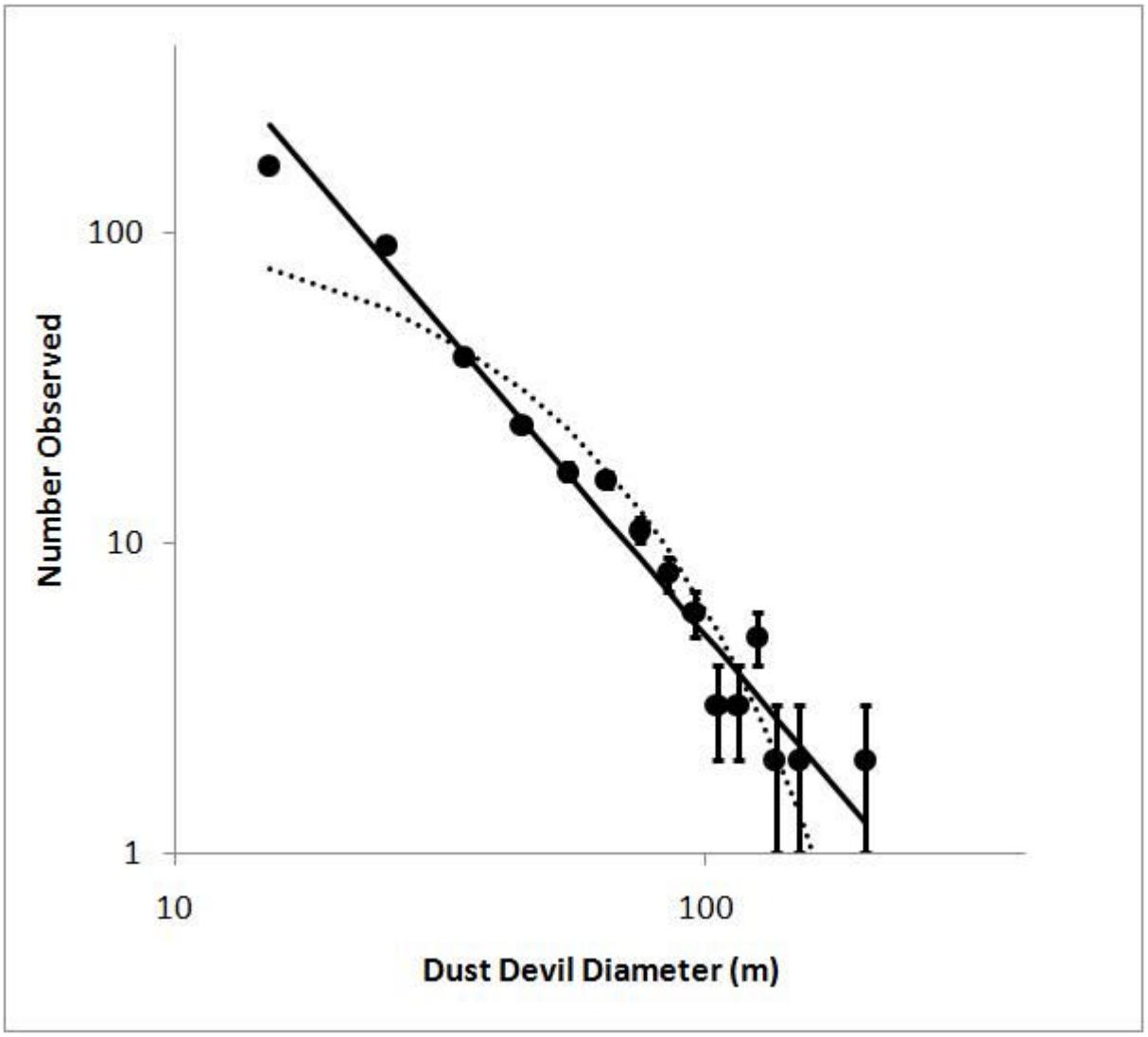

Figure 1. Martian Dust devil counts (4) as filled circles with √N error bars in 10m size bins, except the last 2. Dotted curve is an exponential fit, which is too convex to correctly represent the data: solid line is a -2 power law which follows the trend very well (formal best fit has an exponent of -1.92).

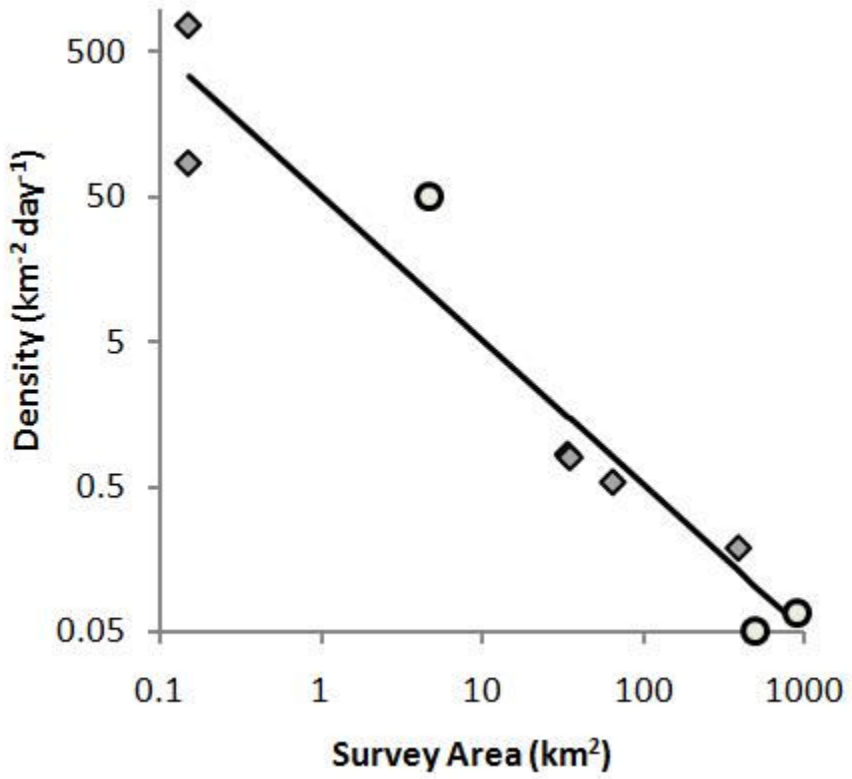

Figure 2. Observed dust devil frequency from surveys on Earth (grey diamonds) and Mars (open circles) – see Supporting Table 1 - as a function of survey area. Solid line is a simple model with Density ($km^{-2}day^{-1}$)=50/Area(km^2), suggesting a solid angle detection threshold and a -2 power law diameter distribution.

Supplemental Table 1

Data from prior dust devil surveys is compiled in table S1 – these data are plotted in figure 2. Note that there are two Gusev surveys – one in which all Navcam images were studied, and a subset which were staring at a nearby spot to measure temporal changes – those two surveys show the same area/density relationship that is indicated by the dataset as a whole.

Ref	Location	Type	Area (km^2)	Number	Density ($km^{-2}day^{-1}$)
S1	Tucson, Arizona	Visual	500	610	0.11
S1	Avra Valley, Arizona	Visual	388	1663	0.19
S2	Mojave Desert, California	Visual	0.15	1151	767.3
S3	Mojave Desert, California	Visual	0.15	156	86.7
S4	White Sands, New Mexico	Visual	64.5	2117	0.54
S4	White Sands, New Mexico	Visual	33.8	1017	0.84
S5	Ares Vallis, Mars	IMP Survey	900	~16	0.07
S6	Gusev crater, Mars	Navcam Survey	~500	533	~0.05
S6	Gusev crater, Mars	Navcam Stare	4.9	351	50
S7	Fowlers Gap, Australia	Visual	33.8	557	0.84

Table S1. Summary of published visual dust devil surveys. IMP is the Imager for Mars Pathfinder. Note the trend of larger areas having smaller densities, even for surveys at the same location.

Supplemental References

S1. Sinclair, P. C. General Characteristics of Dust Devils, Journal of Applied Meteorology, 8, 32-45, 1969

S2. Ryan, J. A., and J. J. Carroll, Dust devil wind velocities: Mature state, J. Geophys. Res., 75, 531–541, 1970

S3. Fitzjarrald, D. E., A field investigation of dust devils, J. Appl. Meteorol., 12, 808–813, 1973

S4. Snow, J. T. and T. McClelland, Dust devils at White Sands Missile Range, New Mexico 1. Temporal and Spatial Distributions, J. Geophysical Research, 95, 13,707-13,721, 1990

S5. Ferri, F., P H Smith, M Lemmon, N O Rennò, Dust Devils as observed by Mars Pathfinder, Journal of Geophysical research, 108, E12, 7-1 to 7-10 doi:10.1029/2000JE001421, 2003

S6. Greeley, R. P. Whelley, R. Arvidson, N. Cabrol, D. Foley, B. Franklin, P. Geissler, M. Golombek, R. Kuzmin, G. Landis, M. Lemmon, L. Neakrase, S. Squyres, and S. Thompson, Active dust devils in Gusev crater, Mars: Observations from the Mars Exploration Rover Spirit, Journal of Geophysical Research, Volume 111, E12S09, 10.1029/2006JE002743, 2006

S7. Oke, A. M. C., N. J. Tapper and D. Dunkerley, Willy-willies in the Australian landscape: The role of key meteorological variables and surface conditions in defining frequency and spatial characteristics, Journal of Arid Environments, 71, 201-215, 2007

Inexpensive Timelapse Digital Cameras for Studying Transient Meteorological Phenomena : Dust Devils and Playa Flooding

Ralph D. Lorenz[1,2,*] and Brian Jackson[2] and Jason W. Barnes[3]

1 Space Department, JHU Applied Physics Laboratory, 11100 Johns Hopkins Road, Laurel, MD 20723

2 Lunar and Planetary Laboratory, University of Arizona, Tucson, AZ 85721

3 Physics Department, University of Idaho, Moscow, ID 83844

* Corresponding author e: Ralph.lorenz@jhuapl.edu t: 443 778 2903 f: 443 778 8939

to be submitted 31st March 2009 as an Article to Journal of Atmospheric and Oceanic Technology

Abstract

We describe the design and performance of timelapse cameras suitable for field deployment in remote locations for long periods and their application to studying two time-variable meteorological phenomena in arid regions, desert dust devils and transient flooding of playa lakes. The camera units (with a total parts cost of ~$80) are based around commercial 'point and shoot' digital cameras, storing ~1500 images on a solid-state memory card over a period between an hour to several months powered by alkaline batteries. A microcontroller can trigger image acquisition based on sensor inputs or at regular intervals. Some example results are presented, showing an association of cumulus clouds with thermals from dust devils, a region of dust enhancement around a dust devil, and a dramatic range of conditions at Racetrack Playa in Death Valley National Park.

1. Introduction

Many phenomena of geophysical or meteorological interest are rare and short-lived, making their observation require expensive effort and patience, or luck. However, developments in consumer electronics – in particular the availability of inexpensive digital cameras with large memory capacity – make it now affordable to deploy self-contained imaging systems in the field that can acquire large numbers of images over long periods.

While this approach does not permit image analysis in real time, but only after the system is retrieved and the data transferred to a computer, it provides scope for considerable savings in labor, in that the observation time can be a large multiple of the deployment time, and the inspection of image data can be performed efficiently in comfortable conditions (or even automatically). Further, the digital image record can permit quantitative analyses with more fidelity and fewer (or at least more quantifiable) biases than visual observation in real time by human observers.

In this paper, we describe a suite of designs of timelapse camera units, and their performance in the field. We consider two applications. First is the study of desert dust devils, dry convective vortices rendered visible by lofted dust (e.g. Balme and Greeley, 2006). These features, a nuisance for outdoor activities and occasionally responsible for structural damage and aircraft accidents (Lorenz and Myers, 2005), typically last only a few minutes. Hot and tedious visual surveys have determined their general diurnal and seasonal pattern of activity, but high-quality data on their sizes, morphologies and recurrence intervals are lacking. Timelapse camera surveys offer the prospect of inexpensively producing strong statistics. A second application relates to the transient flooding of playa lakes. These features are dry for the vast majority of the time, but occasional precipitation can cause them to be water-covered for hours to days. Understanding the occasionally-striking geomorphology of these features requires that their

hydrology be understood. For playas in remote locations, characterization of the playa state (e.g. dry, flooded, frozen or muddy) is most efficiently performed with timelapse observations.

2. Camera Technology

Imaging is a powerful means of obtaining data on many phenomena. In locations with modest infrastructure (AC power and shelter) video surveillance cameras have occasionally permitted interesting geophysical observations. Two examples are particularly interesting. First was the 1995 Kobe earthquake in Japan, wherein the motions of shopping carts relative to the floor was recorded by convenience store security cameras – in this instance the carts were static and the ground motion was what was measured, allowing the fault location and its motion to be inferred (Kikuchi, 1995). A second example was the detection of a meteor fireball by a parking-lot surveillance camera in Nuuk, Greenland (Pedersen et al., 2001) – in fact security camera records have now been used several times to help reconstruct meteorite trajectories.

Video, however, is not convenient for remote observing stations and its frame rate is higher than ideal for many applications. PC-controlled webcams are a good model of the desired capability for many geophysical monitoring projects wherein intervals of minutes or hours can be appropriate, but also require shelter and AC power (although with an internet connection, have the powerful additional ability to be accessible remotely). A modified digital camera can provide webcam-like digital imagery, yet in a compact battery-powered package suitable for field installation. Modern digital cameras, writing to solid-state memory cards with capacities in the hundreds of megabytes or several Gigabytes are now able to store hundreds or thousands of high-quality images – a far cry from the 36-shot reel of 35mm film that was the state of the art for inexpensive cameras two decades ago.

The modifications to the camera are relatively straightforward, although require customization or experimentation for the particular camera model (product turnover in consumer electronics being very rapid, a given model may be discontinued after only a year or two of sales). The principal modification is to trigger the shutter – an internet search for 'hacking cameras' will provide many detailed examples. Some cameras have provision for a cable or infrared remote trigger which can be exploited. More typically, the camera case must be opened and the shutter switch identified. The switch contacts can be bridged, typically by an opto-isolator or a transistor (or conceivably an electromechanical relay) such that an external 5V logic pulse can trigger the shutter. For short intervals between frames (up to say, a minute) a simple 555 timer chip is an inexpensive way of generating regular shutter pulses. While simply 'hotwiring' the shutter this way can allow short timelapse sequences to be acquired immediately after the camera has been turned on, it is typical for cameras to power themselves down after a period of inactivity, this 'auto shut-off' feature typically being employed to save battery energy. Thus it is usual for another switch to have to be activated to wake up the camera.

Because of the need to trigger two switches (and possibly a power relay – see later) and to have arbitrary long intervals between images, we use a small microcontroller to generate the pulses. A variety of devices could be used; we have found the PICAXE-08M (Revolution Education, UK) to be ideal – it can be programmed in a simple BASIC (Beginners All-purpose Symbolic Instruction Code) language, has four input-output lines (allowing, e.g. one for a sensor input, two for camera controls and one for camera power) and costs under $4. Use of a microcontroller allows for substantial flexibility – for simple fixed-delay timelapse work, the interval can be altered in software without making hardware modifications. Arbitrarily-complex image sequences can be constructed (e.g. sets of three images 10 seconds apart, sets to be acquired at 10 minute intervals). Finally, sensor triggered image acquisition can be performed (e.g. to image only when it is windy, or humid, or when a pressure transient suggests the presence of a dust devil e.g. Ringrose et al., 2003. Wagstaff, 2009.) In fact, variants of the arrangement described here are sold commercially as 'trail cameras' for wildlife surveillance. Typically costing $200, these are often

equipped with infrared motion triggers and flashes, to capture images of wildlife at night. Some more expensive timelapse camera installations, based around digital Single Lens Reflex (SLR) cameras, can provide higher-quality imagery, albeit at much higher cost.

We conducted initial experiments with a Flycam-One (ACME OHG, Germany), a small ~$90 camera presumably based around a cellphone camera platform and marketed for use in radio-controlled aircraft. This device records a 640x480 pixel color image to a Secure Digital memory card. The system has four buttons (of which one wakes the camera up, and another triggers the shutter) and uses an internal 3.7V battery. The two switches were bypassed with 2N3904 transistors which were triggered by PICAXE outputs (see figure 1). While there was some initial success, prolonged camera operation using a 4.5V supply (3 AA cells, convenient for driving the PICAXE) caused permanent hardware failure of the memory cards. More elaborate power supply design could avoid problems. It was also found that partial image corruption sometimes occurred with many pixels set to yellow or cyan – although the cause could not be identified with confidence, it never occurred with manual operation of the shutter switch, so it may have been some kind of high frequency noise from the PICAXE. Finally, it was noted that camera operation at voltages below about 3.4V caused soft failure of the memory card (corruption of the filesystem leading to loss of data, but after reformatting the card could be re-used.) Again, careful power supply design might alleviate the problems. During these early experiments, some promising results of observing dust devils, and at Racetrack Playa (Lorenz et al., submitted) were obtained. However, new camera technology became available, with higher-resolution images at a lower camera cost and so experiments with the Flycam were discontinued.

[FIGURE 1 HERE]

New experiments have taken place with the Vistaquest VQ1005 camera. This product comes attached to a keychain and is little bigger than a matchbox. The Visionquest camera is remarkable in being little more expensive ($25) than the 512MB SD memory card on which it can record its images.

The camera takes good-quality pictures at resolutions of 1280x1024 pixels with a CMOS imager with F/2.8 optics, is easy to dismantle and modify, but has some peculiar features, doubtless to keep it both compact and cheap.

Like the Flycam, the VQ1005 stores its images (which it can be at 640x480, 1280x1024 or oversampled at 1600x1200) as JPEG files : typically about 2500 images can be stored on the memory card at the native 1280x1024 pixels. Also like the Flycam, the system does not record an image if the scene is too dark (the VQ1005 will perform auto-exposure between 1/15 and 1/1500 seconds).

The camera is nominally powered by a single AAA cell. When switched on (accomplished by triggering the mode/power switch for 5 seconds) it draws a substantial 800 mA - even a fresh alkaline AAA cell with an open circuit voltage of >1.500 V may drop to 1.47 V. If the supply voltage drops below about 1.45V, the camera powers off. This means only about 10-20% of the total battery energy can be used, compared with the energy to a more typical discharge voltage of 1.2V. A more remarkable (negative) feature of the camera is that even in standby mode, the camera draws about 2mA.

However, it is reasonably straightforward to disconnect the 1.5V battery from the camera using a relay triggered by the microcontroller, such that the standby energy consumption of the camera is reduced to zero. The typical sequence of operations commanded by the microcontroller (connected with 2N3904 transistors to the mode switch and shutter switch, with another transistor driving a relay) is (a) wait desired interval (b) energize relay to connect the 1.5V battery to the camera (c) generate 5 second pulse on mode switch transistor to wake camera up (d) generate 1 second pulse on mode switch to set 1280x1024 pixel mode, or different pulse sequences could be used here to set lower or higher resolution (e) generate 0.5 second pulse on shutter switch to acquire image (f) wait 5 seconds for safe file writing (g) generate 5 second pulse on mode switch to put camera back to sleep. Since the entire sequence takes about 10s, about 2 mA-hr of energy from the 1.5V supply is used. Experiments have shown that a fresh alkaline D-cell, with a nominal capacity of ~20,000 mA-hr, can support about 2500 shuttering sequences,

as long as there is more than a minute between them (it will be recalled that battery capacity depends on discharge rate). This is approximately the number of images that can be stored on a single memory card, although under typical midlatitude conditions only about 1600 images of this number will be recorded, the other ~900 being too dark. If the relay is omitted, such that the camera is always on standby power, only a couple of weeks of operation are possible on an D-cell (regardless how many images are actually acquired.)

For field deployment, the camera is removed from its casing to solder connections to the circuit board for the battery, shutter and mode switch, and mounted with adhesive behind a transparent window in an ABS plastic case. This case also holds the camera battery, the microcontroller/transistor circuit board (an inexpensive 'proto board' is available that is large enough to accommodate the programming connector for the Picaxe and the transistors for camera interfacing) and a separate 3-AA or 3-AAA cell power supply for the Picaxe (see figure 2). The Picaxe uses only a few mA when operating, but in sleep mode (which we use for the interval between images) draws less than 100 microamps, so it can operate for many months on the ~1000 mA-hr available from AA cells. To minimize visual impact in the field, the case was sprayed with textured earth-toned paint.

[FIGURE 2 HERE]

As described in the subsequent two sections, the cameras appear to have functioned adequately at least a few degrees below freezing, and at temperatures of 40 C or more. The major difficulty encountered, in trials not reported in the following sections, has been unexpected data corruption associated with battery undervoltage. This has been successfully mitigated by several approaches. The microcontroller can compare its supply voltage with a reference, and veto image acquisition if the voltage drops unacceptably. A regulated supply is an alternative (the Vistaquest camera normally uses a single AAA cell, so regulating the 4.5V microcontroller supply to 1.5V using an adjustable regulator such as LM317 is an effective, if slightly energy-inefficient approach). Finally, a simple strategy is simply to use

a fresh set of batteries each mission and limit the camera to acquire a fixed number of images (known empirically not to cause the voltage to drop) and then stop. There is of course a tradeoff between extracting the maximum number of images possible with a given energy source, and the effort one is prepared to devote to the challenge : this tradeoff determines which of the above approaches is adopted.

3. Application to Dust Devil Surveys

Dust devils are desert whirlwinds rendered visible by lofted dust. While field surveys (e.g. Sinclair, 1969; Fitjzjarrald, 1973; Snow and McLelland, 1990 ;Oke et al., 2007) agree on the diurnal pattern of activity, the absolute numbers of dust devils in surveys vary widely, possibly as a result of different detection thresholds among the observers and the strong increase in number of smaller dust devils. In that connection, while a truncated exponential size distribution has been advocated on the basis of the crudely-binned size statistics obtained by visual observers (Kurgansky, 2006), higher-quality data is needed to discriminate such an exponential description from, for example, a power law.

Dust devils can occur in a variety of morphologies (e.g. Balme and Greeley, 2006) – wide cones to tall, slender columns to irregular. Columns may tilt appreciably due to wind shear, and the dust devil as a whole may move at a speed different from the ambient wind. Correlation of these morphologies with meteorological conditions has so far been only anecdotal, and is complicated by the fact that an individual dust devil may evolve in shape and speed which may confound a field observer's efforts to classify the dust devil quantitatively. A timelapse camera survey would allow robust statistics on these aspects of dust devils to be compiled, and related to ambient meteorological conditions.

Finally, it has been suggested that there may be a short-term periodicity in dust devil occurrence (of the order of 20 minutes), perhaps due to activity draining the near-surface boundary layer of the hot air that powers the devils, or perhaps to some feedback involving lofted dust. However, visual surveys to

date have generally only recorded statistics of dust devils in 1-hour time bins, making detection of such periodicity impossible.

As a trial, we set up a single Flycam-based camera near Gates Pass in Tucson, looking westwards towards the Avra Valley area surveyed by Sinclair (1969). This camera was set to record a 640x480 pixel image every minute. Although the valley was some 10 km away, several large dust devils were detected. Meteorological conditions were sufficiently humid that although a hot and overall dry day, lofted air was able to condense, and intriguingly small cumulus clouds formed contemporaneously and almost directly above several dust devils – see figure 3.

[Figure 3 here]

A second trial was performed in May 2008, with a Visionquest camera set to acquire images at 45 second intervals. This camera was set up near the Arizona Desert Museum, and thus is rather closer to the Avra Valley plain where the dust devils form. An example set of images is shown in Figure 4 and nicely shows the progression of a dust devil across the scene at a more or less constant velocity. The fixed location means that few features in the image change from one frame to the next, and illumination changes only slightly. Thus successive images can be differenced in post-processing, or the average frame from a batch of images subtracted from each, to leave the changing portion of the image – in this case the dust devil. This approach has been used on sequences of images to detect dust devils observed on the surface of Mars by the rover Spirit (Greeley et al., 2006). It is seen in figure 4 that in addition to the dust devil itself, there is a broader region of dustiness, perhaps either disturbed by the radial flow into the dust devil or even dust lofted by the devil and ejected at its top.

Although not shown in figure 4 (where the images have been cropped to the region of interest containing the dust devil), the differenced images showed a quite clear motion in the sky, even though no clouds were apparent in the raw images, or to a human observer. The contrast enhancement provided by

differencing evidently made visible small amounts of cloud or dust opacity that could act as wind tracers in the sky.

[Figure 4 here]

Clearly, then, the instrument described here can be used for systematic surveys, and in principle can have a lower opacity threshold than might a fatigued human observer. A variety of field observing strategies are possible. In a typical deployment, one might spend an hour deploying several (e.g. ~4) cameras at the beginning of the day, then an hour retrieving them at the end of the day, and an hour to download and study the images. Even a manual inspection of such an image sequence is an efficient approach in that one can browse through an image sequence at one frame every second or so. Additionally, there are now machine vision algorithms developed for real-time dust devil detection on the Mars Exploration Rovers (Castano et al. 2008) that can automatically process images and identify those that contain dust devils. Thus for ~three hours of effort, one obtains ~36 station-hours of observation – an effective force-multiplier.

Another approach might be to set up cameras to record for 5 days, with a cadence of 1-2 minutes. This provides an even higher force-multiplier for the effort, at the expense of poorer time resolution (resulting in ambiguity of discriminating long-lived but moving devils from separate but short-lived devils). Even if the interval between images is longer than the typical lifetime of an individual dust devil and thus is an incomplete census, a regularly-spaced image sequence still provides an unbiased means of evaluating the variation with time of dust devil numbers, size, dust loading and morphology and the correlation between these variables. The combination of such data with meteorological context measurements, and desirably with in-situ measurements of the dust devils themselves, would be particularly useful.

4. Playa Lake Observations

Observing dust devils was the principal motivation behind developing these cameras. However, dust devil activity is minimal during winter, and thus a second application was found to field-test the camera during the winter months. This relates to the transient flooding of Racetrack Playa in Death Valley National Park. This is a 4.5x2 km lakebed at an elevation of 1130m and may be wetted only for a few days during a typical year, since the park as a whole is very dry (Roof and Callagan, 2003). In this respect (and several others) it may resemble some lakes on Saturn's moon Titan (Lorenz et al., submitted, 2009b), where evaporation also exceeds precipitation by orders of magnitude, although on that cold, distant world the fluid being rained and evaporated is methane (e.g. Lorenz and Mitton, 2008). It is exceptionally flat (the south end is only a few cm lower in elevation than the north) and is of mixed sand-silt-clay composition, usually with striking but small dessication polygons. It is distinguished (e.g. Sharp and Carey, 1976) by the presence of some dozens of rocks (usually cobbles or small boulders) which are very distinct against the very uniform playa (figure 5), and often appear at the end of trails or furrows in the playa surface. These trails suggest that the rocks have moved across the surface at some speed when the playa was wet. Much attention has been directed towards documenting the rocks and their movements (e.g. Kirk, 1952; Sharp and Carey, 1976; Reid et al., 1995; Messina and Stoffer, 2000), apparently caused by wind, possibly facilitated in some instances by ice formations around the rocks. However, in-situ meteorological data at the playa (reached by a sometimes-closed 25-mile dirt road) is not available and observations of how frequently the playa is flooded, muddy or frozen are lacking.

[Figure 5 here]

Since Racetrack Playa is a site of outstanding natural beauty, and formally a Wilderness Area, equipment must therefore be inobtrusive, and set up off the playa itself. After approving the location of our camera with National Parks Service staff and acquiring the necessary permit, we performed an initial trial with a C-cell powered Flycam system. This was packaged in a black die-cast aluminium box 6x12x20cm and

set in the cliffs at the south end of the playa. Over the observation period from 29th November 2007 to 3rd March 2008 some 1100 images were acquired with a nominal spacing of 1 hour. Some images were partially corrupted by a filesystem problem with low-voltage operation of the SD memory card to which the images were recorded, but the state of the playa could nonetheless be evaluated and three episodes of wetting were noted (Lorenz et al., submitted).

A subsequent observation was performed with a Vistaquest camera between 3rd December 2008 and 3rd March 2009, with an interim changeout of the camera allowing a higher frame rate of ~2/hr. Image quality was much better than for the flycam, with no significant image corruption, as well as higher intrinsic resolution. About a half dozen images were truncated, perhaps due to issues with low-temperature operation. The color balance was also suspect on one image (the overall appearance was pink) : this is likely due to poor performance of the automatic color balance in the camera in marginal dawn lighting conditions when the scene was white with snow.

For most of the observing period, the playa had its usual dry condition, with one brief dusting of snow circa . However, a more significant snowstorm passed through at the beginning of February, 2009 (figure 6) and indeed some falling snowflakes appear, slightly blurred, in some images. One difficulty arises in variable weather conditions in that the images are not time-stamped – one must infer an approximate date and time from the image filename (corresponding to the ordinal number of the file being written to the memory card). In other words, image #0145 occurs between #0144 and #0146, and probably occurs 30 minutes (or whatever delay is implemented in the microcontroller) after #0144. However, if darkness caused by time of day, or by heavy cloud, brought the camera below the threshold at which it stores an image, there will be an undetermined number of image intervals between successive recorded image files (in a sequence of geological layers, the analogous discontinuity would be called an unconformity.) Thus dates cannot always be determined with absolute precision, although we know from humidity and temperature measurements acquired with nearby dataloggers that were equipped with

timestamps that conditions became suddenly humid, and buffered around the freezing point, suggesting the presence of snow, on February 6th, 2009.

[Figure 6 here]

Subsequent images show that the snow melts and the resultant shallow lake on the playa can be blown significantly by the wind (figure 7) – so-called 'wind set up' and the surface of the lake can be roughened significantly (figure 8) providing second indication in the image record of wind stress.

[Figure 7 here]

[Figure 8 here]

The following morning, the lake could be seen to be frozen (figure 9). The lake texture was slightly different in the images from how it appeared when wind-ruffled, but more robustly the features on the lake surface remained identical in several frames spanning a couple of hours, before they progressively disappeared through melting. Determining the lake to be frozen places a constraint on its energy budget, as well as being of potential interest in the motion of the rocks on the playa in that ice sails may facilitate wind dragging on the rocks. Later that day, the ice had melted, and wind stress on the lake was evidently minimal – the lake surface became a perfect mirror (figure 10)

[Figure 9 here]

[Figure 10 here]

Finally, the progressive evaporation of the lake could be seen allowing constraints to be placed on the overall evaporation rate – in essence the lake acts as a large, natural evaporation pan. Given the present California drought, independent measures of evaporation rate may be of interest. Intriguing semi-regular patterns formed in the playa bed (figure 11), as drying of the playa became complete. Whether these patterns are purely ephemeral and stochastic, or reflect some underlying (but invisible) variation in

the character of the playa sediments cannot be determined, although repetition of the patterns on a subsequent wetting/drying cycle would support such a substrate control of the pattern.

[Figure 11]

Of course, it would be interesting to observe the rocks themselves in actual motion (and we note that the cameras used here are able to record short video sequences as well as stills – in the case of the Visionquest camera, it would require only an additional couple of mode switch pulses in the microcontroller program). However, given that the rock movement episodes are only ~10s in duration, and surveys have indicated (e.g. Sharp and Carey, 1976) that movements may take place perhaps one year in three, movement occurs only about one millionth of the time. Thus observations while rocks are in motion would likely require some kind of wind-triggered imagery : there is a fair probability that movement might in any case occur unobservably at night, and that the conditions that cause movement (wet and wind) may tend to cause obscuration of the playa by spray or fog. However, regular imagery can at least permit the time of a movement event to be documented to a day or better, thereby allowing the conditions pertaining when the event occurred to be documented. Further, as we have shown here, imaging also permits the frequency and duration of various conditions (wet, frozen, etc.) of the playa to be quantified.

5. Conclusions

The memory capacity, low cost and small size of digital cameras now permits large amounts of image data to be acquired in settings that were not previously feasible. Timelapse imagery need not be acquired from fixed sites, but can be taken through the windows of road vehicles or aircraft, or even from

kites or balloons. From fixed sites, as described here, these inexpensive devices can open new windows into the study of time-variable meteorological phenomena.

Acknowledgements

This work was funded in part by the NASA Applied Information Systems Research (AISR) program. BJK acknowledges a research grant from the Geological Society of America, and discretionary support from the Director of the Lunar and Planetary Laboratory, University of Arizona. We thank David Choi, Catherine Neish and Joe Spitale for assistance in the field. We are grateful for the assistance of David Ek, Wilderness Resources Coordinator at Death Valley National Park in conducting the field observations.

References

Balme, M. and R. Greeley, Dust Devils on Earth and Mars, Reviews of Geophysics, 44, RG3003, 2006

Castano, A., A. Fukanaga, J. Biesadecki, L. Neakrase, P. Whelley, R. Greeley, M. Lemmon, R. Castano, S. Chien, Automatic detection of dust devils and clouds on Mars, Machine Vision and Applications, 19, 467-482, 2008.

Fitzjarrald, D. E., A field investigation of dust devils, J. Appl. Meteorol., 12, 808–813, 1973.

Greeley, R. P. Whelley, R. Arvidson, N. Cabrol, D. Foley, B. Franklin, P. Geissler, M. Golombek, R. Kuzmin, G. Landis, M. Lemmon, L. Neakrase, S. Squyres, and S. Thompson, Active dust devils in Gusev crater, Mars: Observations from the Mars Exploration Rover Spirit, Journal of Geophysical Research, Volume 111, E12S09, 10.1029/2006JE002743, 2006

Kikuchi, M. A shopping trolley seismograph, Nature, 377, 19, 1995

Kirk, L. G. 1952. Trails and rocks observed on a playa in Death Valley National Monument, California. Journal of Sedimentary Petrology, 22, 173-181.

Kurgansky, M. V., Steady-State properties and statistical distribution of atmospheric dust devils, Geophysical Research Letters, 33, L19S06, doi:10.1029/2006GL026142, 2006

Lorenz, R. D. and J. Mitton, Titan Unveiled, Princeton University Press, 2008.

Lorenz, R. D. and M. J. Myers, Dust Devil Hazard to Aviation: A Review of US Air Accident Reports, Journal of Meteorology, 30, 299, 178-184, 2005.

Lorenz, R. D., B. Jackson and J. W. Barnes, Meteorological Conditions at Racetrack Playa, Death Valley National Park : Implications for rock production and transport, Journal of Applied Meteorology and Climatology, submitted

Lorenz, R. D., B. Jackson and A. Hayes, Racetrack and Bonnie Claire : Southwestern US Playa Lakes as Analogs for Ontario Lacus, Titan, Planetary and Space Science, submitted.

Messina, P. and P. Stoffer 2000, Terrain analysis of the Racetrack Basin and the sliding rocks of Death Valley, Geomorphology, 35, 253-265.

Oke, A. M. C., N. J. Tapper and D. Dunkerley, Willy-willies in the Australian landscape: The role of key meteorological variables and surface conditions in defining frequency and spatial characteristics, Journal of Arid Environments, 71, 201-215, 2007

Pedersen, H., R. E. Spalding, E. Tagliaferri, Z. Ceplecha, T. Risbo and H. Haack, Greenland superbolide event of 1997 December 9, Meteoritics and Planetary Science, 36, 549-558, 2001

Reid, J. B., Bucklin, E. P., Copenagle, L., Kidder, J., Pack, S. M., Polissar, P. J., and Williams, M. L. 1995. Sliding rocks at the Racetrack, Death Valley: What makes them move? Geology, 23(9): pp. 819-822.

Ringrose, T. J., M.C. Towner, and J.C. Zarnecki, Convective vortices on Mars: a reanalysis of Viking Lander 2 meteorological data, sols 1–60, Icarus 163, 78–87, 2003

Roof, S. and C. Callagan, The Climate of Death Valley, California, Bulletin of the American Meteorological Society, 1725-1739, December 2003

Ryan, J. A., and J. J. Carroll, Dust devil wind velocities: Mature state, J. Geophys. Res., 75, 531–541, 1970

Sharp, R. P. and Carey, D. L. 1976. Sliding Stones, Racetrack Playa, California. Geological Society of America Bulletin, 87: pp. 1704-1717.

Sinclair, P. C. General Characteristics of Dust Devils, Journal of Applied Meteorology, 8, 32-45, 1969

Snow, J. T. and T. McClelland, Dust devils at White Sands Missile Range, New Mexico 1. Temporal and Spatial Distributions, J. Geophysical Research, 95, 13,707-13,721, 1990

Wagstaff, K., Real-Time Detection of Dust Devils from Pressure Readings, NASA Tech Briefs, 22-23, March 2009

Figures

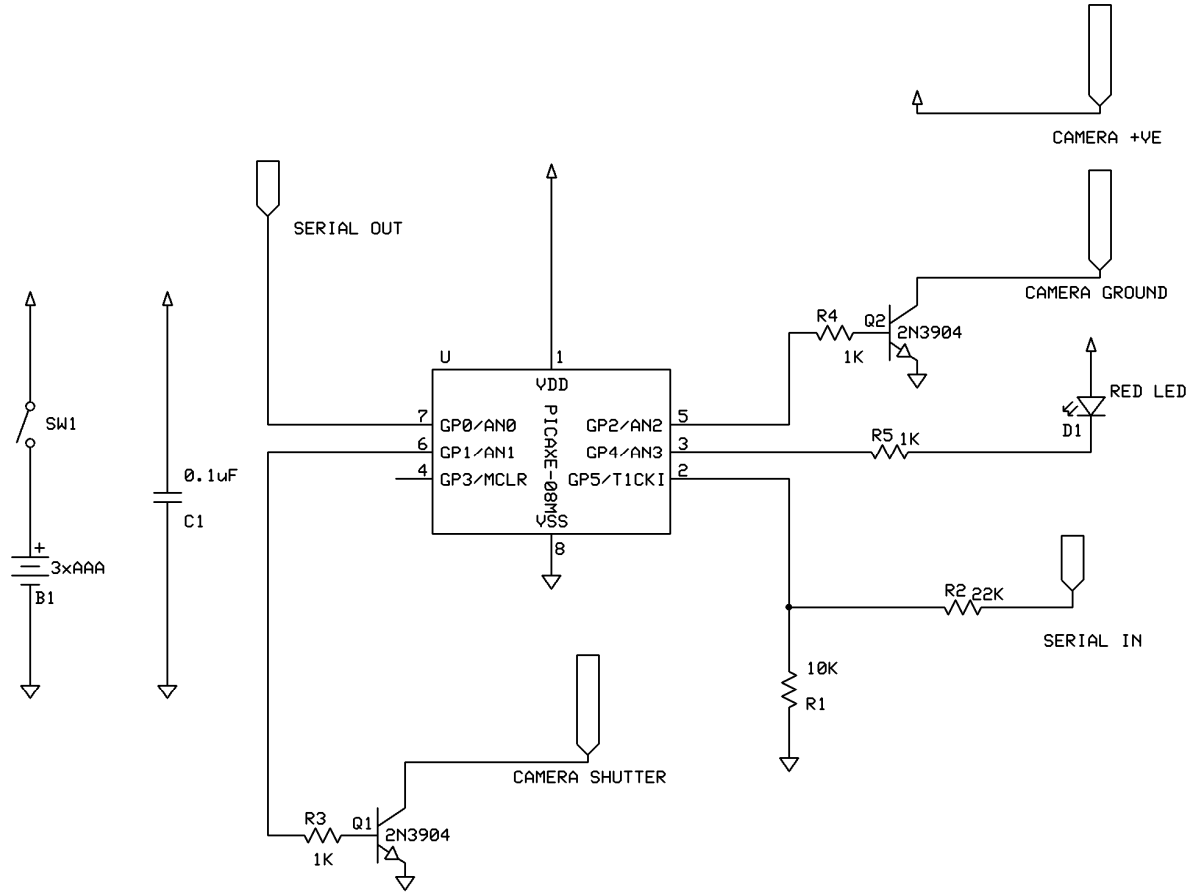

Figure 1. Circuit for the flycam trigger (the basic circuit for the VQ1005 is identical). The serial in and out connections are to permit programming of the Picaxe chip. The indicator LED is optional – that pin on the microcontroller can instead be used for a sensor input to trigger camera operation.

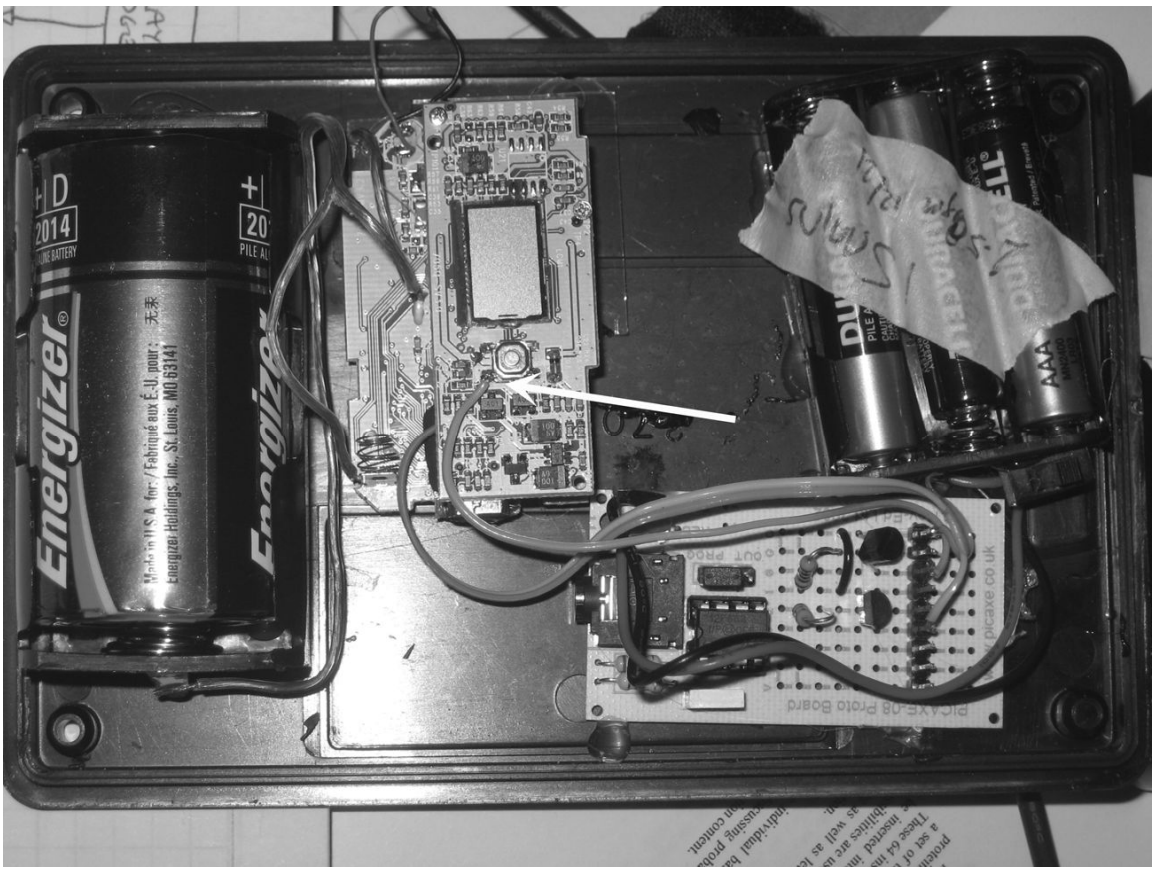

Figure 2. Layour of VQ1005 camera unit. At left is alkaline D-cell to power camera. Next is camera itself (case removed, so circuit boards are exposed, showing LCD status display. A wire to the mode switch terminal from the microcontroller board is arrowed. At lower right is the microcontroller board with switching transistors, and above that the 3-AAA cell power for the microcontroller.

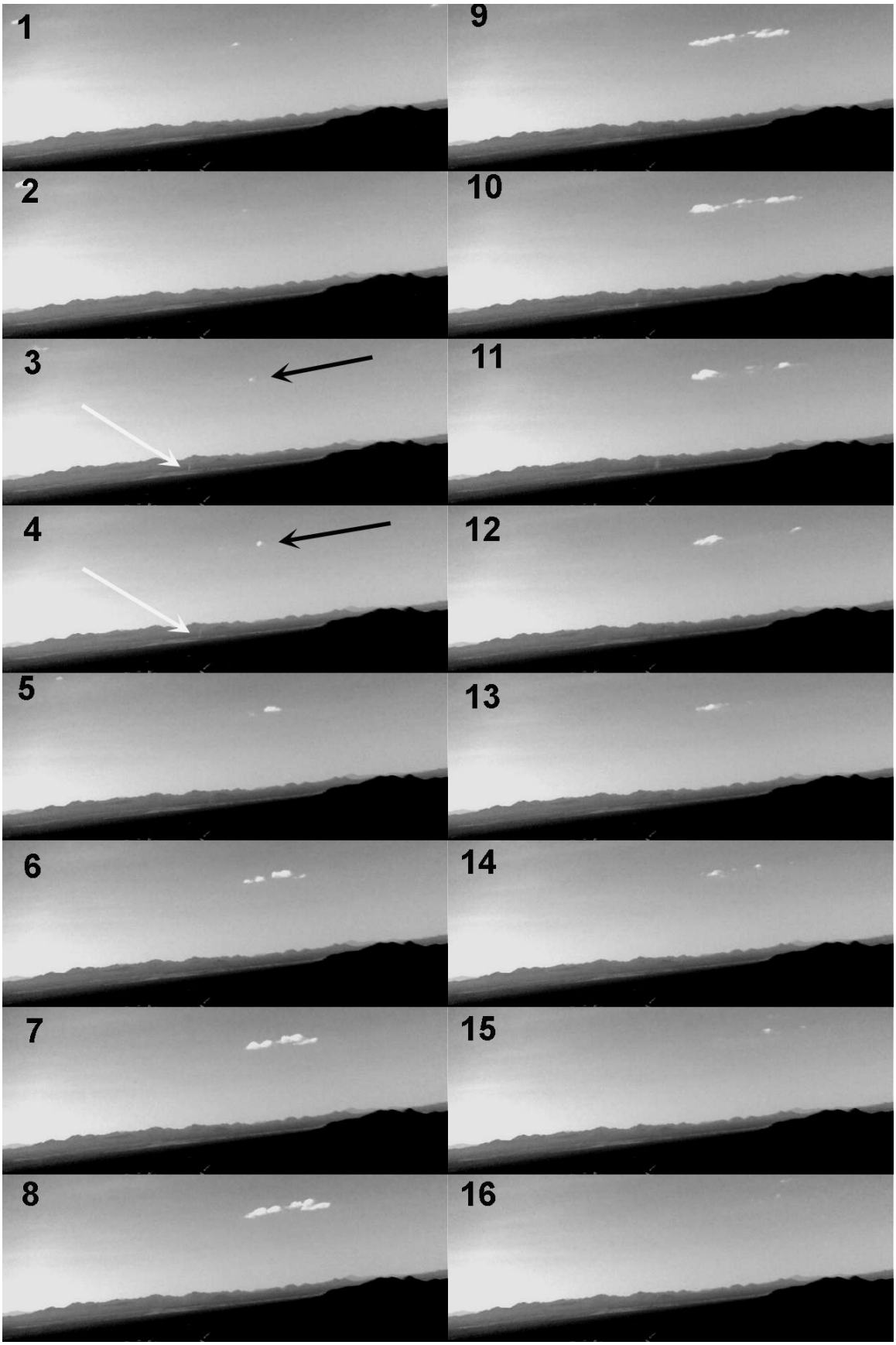
1
2
3
4
5
6
7
8
9
10
11
12
13
14
15
16

Figure 3. A sequence of 16 images spaced by ~1 minute at Gates Pass, nr Tucson, AZ, looking west to Avra Valley. Sequence begins at ~1430 hrs on 18th September 2007. Note the formation of small cumulus clouds (black arrow), apparently by thermals associated with a dust devil (white arrow).

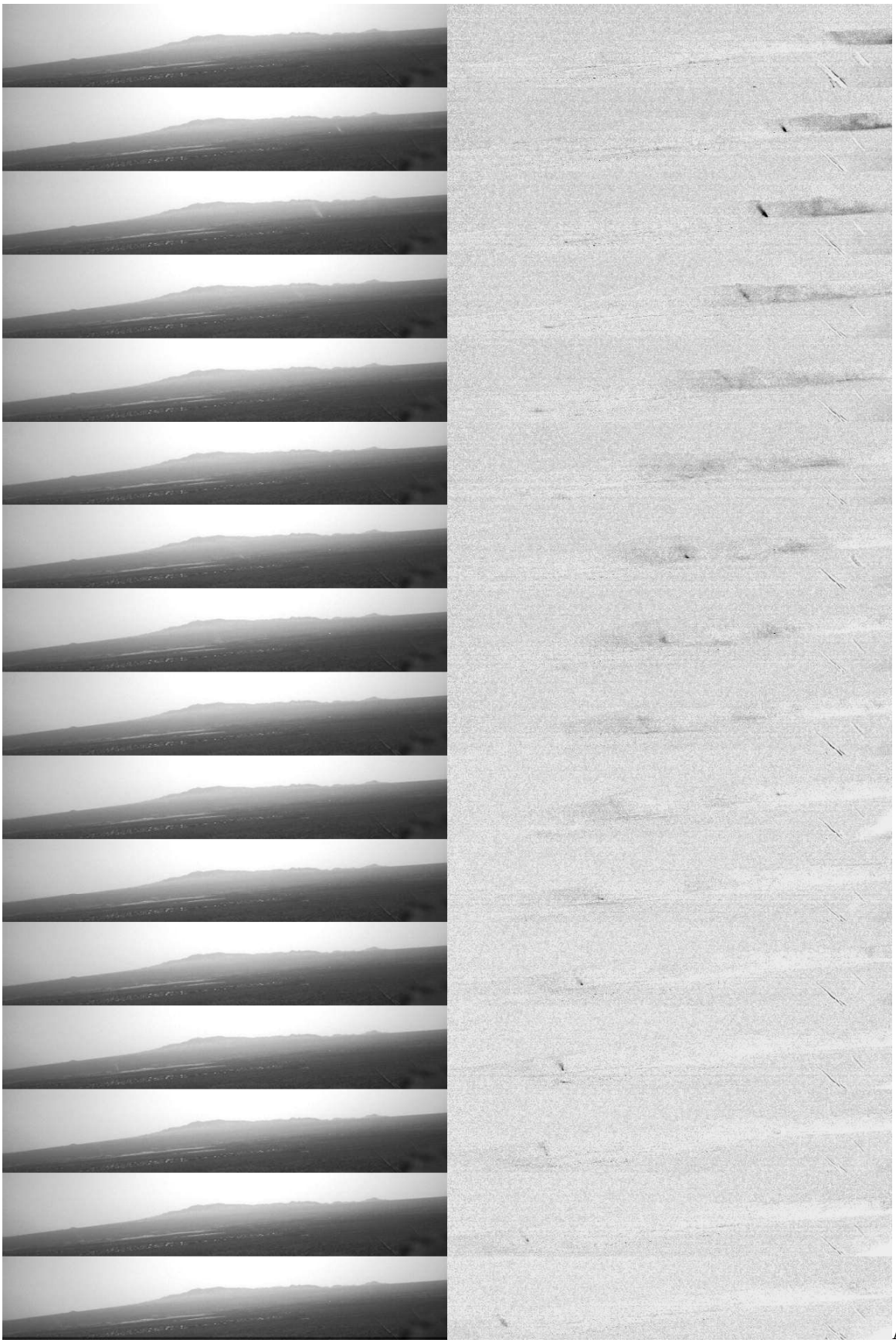

A

Figure 4. A sequence of cropped images, 45s apart, acquired in Avra Valley (looking Southwest) starting at 13.05 hrs on 20 May 2008. At right is the same sequence, but showing only the difference between each image and the average of the set, thereby enhancing the changing feature – specifically the dust devil, which is visible in the difference image for nearly the entire set, whereas it is only prominent in the originals in a few frames. Notice the consistent motion across the scene and the variable strength of the devil itself (which would be difficult to characterize quantitatively by eye). Note also the broad perturbation around the devil – presumably lofted dust. The persistent line diagonal line at right is a blade of grass in the foreground which is moved by the wind and thus appears in difference images.

Figure 5. The normal condition of Racetrack Playa. Image 384, acquired in late January 2009, looking north from the cliffs above the south edge of the playa. The rock formation 'The Grandstand' is visible two thirds of the way from left to right, just above the horizontal edge of the playa half way up the image. Five rocks on the playa are visible in the foreground.

Figure 6. The playa after a snowstorm. Image 445. Note that the snow cover on the playa itself is rather thin, as the cover of the playa mud can be discerned.

Figure 7. Image 476. The snow has melted and the playa is partly covered with water. The playa is exposed at left, and a narrow band of smooth water is evidenced at the edge by a mirror-like reflection of the distant skyline. To the right, the water surface is disturbed by wind.

Figure 8. Image 477 – about 30 minutes after figure 7. The playa is completely flooded, although the surface is disturbed by wind (individual ripples can be discerned at lower right). It seems likely that wind stress on the surface of the shallow lake (it is not so deep as to submerge the ~20cm rocks in the foreground) pushes the water around, exposing the bed at the upwind side.

Figure 9. Image 490 – early the day following Figure 8. The surface of the playa lake is frozen (the surface patterns are identical in several subsequent frames, confirming that the textures are fixed and therefore due to ice, rather than wind effects.)

Figure 10. Image 504, late in the same day as figure 9. Conditions are evidently calm, as evidenced by the near-perfect specular reflection on the lake surface.

Figure 11. Image 553, a few days after figure 10. Evaporation has nearly dried the lake out and the residual moisture forms semi-regular patterns on the playa surface. The water or frost highlights some subtle playa textures, notably the parallel lines about 2/3 across the image delineating a rock trail.

Meteorological Conditions at Racetrack Playa, Death Valley National Park : Implications for rock production and transport

Ralph D. Lorenz[1,2,*], Brian Jackson[2] and Jason W. Barnes[3]

1 Space Department, JHU Applied Physics Laboratory, 11100 Johns Hopkins Road, Laurel, MD 20723

2 Lunar and Planetary Laboratory, University of Arizona, Tucson, AZ 85721

3 Physics Department, University of Idaho, Moscow, ID 83844

* Corresponding author e: Ralph.lorenz@jhuapl.edu t: 443 778 2903 f: 443 778 8939

submitted 13th December 2008 as an Article to Journal of Applied Meteorology and Climatology

Abstract

We report an analysis of weather records at several stations near Death Valley National Park, in an attempt to gauge the frequency of conditions which can erase, or more rarely form, the famous trails in the mud of Racetrack Playa. These trails are formed by rocks moved by strong winds, but first require the playa to be wet, which occurs typically for only a few days in any given year. Freezing conditions, which are instrumental in generating the rocks, and may facilitate their transport, occur at the playa around 50 nights a year. Using measurements acquired in-situ over winter 2007-2008 we show that nearby stations offer a useful, albeit imperfect, proxy for conditions at the remote playa.

1. Introduction

Racetrack Playa in Death Valley National Park, California is a 4.5x2 km lakebed at an elevation of 1130m, only occasionally flooded. It is exceptionally flat (the south end is only a few cm lower in elevation than the north) and is of mixed sand-silt-clay composition, usually with striking but small dessication polygons. It is distinguished (e.g. Sharp and Carey, 1976) by the presence of some dozens of rocks (usually cobbles or small boulders) which are very distinct against the very uniform playa (figure 1), and often appear at the end of trails or furrows in the playa surface. These trails suggest that the rocks have moved across the surface at some speed when the playa was wet.

[FIGURE 1 HERE]

Much attention has been directed towards documenting the rocks and their movements (e.g. Kirk, 1952; Sharp and Carey, 1976; Reid et al., 1995; Messina, 1998), and to speculating upon the mechanism by which they are induced to move, presumably by wind, e.g. Schumm (1956). While Sharp and Carey (1976) dismiss study of the playa rocks as 'hardly matters of greatest scientific import' before going on to present a rather detailed investigation motivated by 'broad interest in this curious phenomenon', we argue that in fact the rocks are of interest from a process perspective – they are Quarternary geology in action. The peculiar circumstance of isolated rocks moving on a playa represents a rare combination of rock supply, transport and destruction, all of which are controlled by meteorology.

In order to understand the rock movements, it would be desirable to know several key meteorological variables. However, the playa's isolated location (away from communications infrastructure as well as from habitation) and more importantly its deserved status as a site of extreme

natural beauty (and more formally as a protected Wilderness site within the National Park) mean there have been no systematic weather records acquired in the past at the playa itself.

In this study, we analyse records from sites close enough to the playa to be affected by the same weather systems, and spanning a range of elevations to assess the likely conditions at the playa and identify easily-available proxy measurements that might indicate conditions that permit rock-moving. We validate these proxy studies with some limited in-situ data acquired at the playa, with National Park Service concurrence, over the winter 2007-2008.

2. Meteorological Variables of Interest

Three principal sets of data are of interest : precipitation, temperatures and wind. The need for precipitation knowledge is evident – the playa must be wet to reduce the friction between the rock and the playa surface in order for the rocks to move, and the excavation of trails in the playa material requires that it is soft.

It is important to consider temperatures for several reasons. First, it seems likely that at least some episodes of rock movement take place when rocks are mechanically linked by a sheet of ice (since tracks – even with many turns – can be parallel.) The debate (e.g. Reid et al., 1995) as to whether freezing is actually *required* (by enhancing the area over which wind drag can act) for movement is not important here. A second issue is that the rocks predominantly break off from the dolomite cliffs at the south end of the playa, and freeze-thaw cycling is a likely mechanism for their formation (e.g. Bland and Rolls, 1998). Accordingly the number of freeze-thaw cycles encountered at the playa is of interest in controlling the rock supply, and perhaps also in controlling the ultimate destruction of the rocks. Finally, air temperature also influences evaporation rate and thus the longevity of wetness on the playa.

Finally, wind (and in particular peak wind) is of most interest, but is the most challenging variable upon which to acquire useful insights. Messina and Stoffer (2000) investigate the role that the local steep topography around the playa may play in focusing the wind speeds and directions on the playa itself. Given that the gusts moving the rocks may be of very short duration, and indeed may be peculiar to the playa itself, the data from nearby sites will only serve as a guide. Furthermore, since the flat playa has very low aerodynamic roughness, it may be that the boundary layer is particularly slim, exposing the rocks to higher winds than might be expected elsewhere for a given windspeed recorded at a typical anemometer height.

However, while the peak speeds recorded at nearby stations will only provide some guidance as to whether a given day had strong winds, the overall statistics of wind direction are important in that to understand the residence time of rocks on the playa in stochastic models of rock migration (trails have been found going north-south as well as south-north – e.g. Stanley, 1955) we require knowledge of the relative frequencies of northerly and southerly wind, which are likely to correlate at least somewhat with regional winds (see discussion in Messina and Stoffer, 2000). Finally, wind controls evaporation rate and thus how long the playa stays wet after a precipitation event.

3. Data

We obtained daily summary RAWS (Remote Automatic Weather Station) data from the Western Regional Climate Center (http://www.raws.dri.edu/wraws/scaF.html) . These stations, listed in table 1, are operated by various agencies, but most particularly the Bureau of Land Management.

The RAWS data give a daily summary including average wind speed and direction, gust speed, air temperature (maximum, minimum and average) relative humidity (maximum, minimum and average),

solar fluence (kW-hr/m^2) , precipitation and an estimate of Penman evaporation. The RAWS datasets vary in extent, with start dates from 1988 to 1995 running through the present. A few data gaps exist, especially solar fluence and winds, and thus also the derived Penman evaporation. We take these gaps into account when computing our statistics.

[TABLE 1 HERE]

There are additional weather stations in the area which we have not considered since they are generally much less complete and/or extensive. The nearly century-long weather record at the resort at Furnace Creek has been discussed by Roof and Callaghan (2003), which gives a useful overview of the climate of Death Valley. There is a NOAA USCRN (US Climate Reference Network) station at Stovepipe Wells (see figure 3) which for which on-line data is available (http://www.ncdc.noaa.gov/crn/hourly?station_id=1105) but not all the meteorological variables of interest are recorded in convenient form. Finally, several personal weather stations, as well as those at airfields, are situated in the Ridgecrest/Inyokern/China Lake area (a selection may be viewed at e.g. www.wunderground.com), but since these are very close to the Indian Wells Canyon RAWS site in our dataset, they yield little additional information.

3. Results

3.1 Precipitation

As is typical for desert regions, the precipitation is zero for long periods of time, punctuated by occasional downpours that deposit often upwards of 10mm of rain. Rain can of course be highly localized, e.g. Roof and Callagan (2003) report an occasion where 3.8cm of rain fell in 20 minutes at Cow Creek (the National Park Service offices), yet no rain was detected at Furnace Creek only 5km to the south and at a similar elevation.

An inspection of the precipitation records (Figure 4) suggests that the area may experience a periodic variation in the occurrence of the heaviest downpours – circa 1990, 1996-1997 and 2002-2003 and the present seem to have fewer heavy precipitation events.

[FIGURE 4 HERE]

Figure 5 plots the annual mean precipitation at the various sites as a function of elevation. It is seen that at the playa's elevation of 1130m, precipitation of 150mm is typical.

[FIGURE 5 HERE]

For the purpose of enabling rock movement, of interest is the length of time for which the playa remains wet (and thus slippery). As a crude metric, we take the daily precipitation records for the RAWS stations, and when an event occurs, we set the depth of water on the playa to that value, then progressively decrement the depth by the daily Penman evaporation computed in the RAWS record, until the depth becomes zero. This procedure must be considered only a guide, since the playa water depth may exceed the precipitation by a factor of a few due to the larger catchment area that drains into the playa (with some uncertain amount of infiltration into the soil) , and winds and thus the resultant evaporation rate at the playa may differ from any given site.

Figure 6 shows the results. Typically a site will dry out within one or two days, and in very rough terms the probability in a given year of seeing an event when the playa remains wet for N days is ~1/N.

[FIGURE 6 HERE]

3.2 Temperatures

While Death Valley is justifiably famous for its dryness and high peak daytime temperatures (e.g. Roof and Callaghan, 2003), it commonly sees low winter temperatures. Further, the overall dryness means that the dry adiabatic lapse rate of 10K/km (rather than a wet value of ~5K/km) applies and thus elevated areas see even colder conditions than might otherwise be expected. The average temperatures are not of especial interest in this study, but the number of occasions on which freezing occurs is, both for considering the probability of the flooded playa freezing over, and for controlling the freeze-thaw production and destruction of rocks.

Figure 7 shows the average number of nights a year that the various stations experience freezing conditions – a clear trend with altitude is seen, with the number of freezing nights increasing by about 1 night per year per 12m of elevation rise from ~1100m. However, freezing conditions are controlled substantially by the micrometeorology of a given site, and the playa likely sees freezing conditions rather more frequently than this trend would indicate (as indeed we ourselves measure in-situ at the playa – see later).

First, the solid angle of cold, clear desert sky seen from a site determines how effectively it cools radiatively at night – nearby terrain or vegetation will reduce the probability of freezing. On the other hand, terrain obstruction, especially to the south, will reduce the amount of direct sunlight available to warm a surface during the day. Further, local topographic minima will act as sumps for cold air (this is likely the explanation for the outlier data point – Mojave River Sink (6) in figure 7. Thus wide but closed basins like Racetrack Playa combine the pooling of cold air with an overall good view of the cold sky,

while the cliffs and hills to the south-east put much of the playa in shadow for much of the day during winter. Thus Racetrack Playa behaves somewhat as a cold air pool (a more extreme example of which, reaching record temperatures of -56^{o}C, is the 1km-wide Peter Sinks basin in Utah – see Clements et al., 2003.)

[FIGURE 7 HERE]

3.3 Winds

We plot wind rose data from the RAWS sites in Figures 8 and 9, the latter considering only the faster winds (>5m/s). It can be seen that in general (with biases due to the local topography evident in the map) winds come predominantly from the south or west. The principal exception is the Oriental Wash site (site 2, the northernmost on the map) where winds often come from the northeast, entering the valley at that end and flowing south. In fact, it is well-known that it is the convergence of this flow with the more general flow from south and west is what leads to the deposition of the sand to form the dunes at Stovepipe Wells.

[FIGURE 8 HERE]

[FIGURE 9 HERE]

It has been informally observed on our several visits to the playa that the wind has been from the south to north, a pattern also noted by Messina (1998). The rock trails mapped by Messina, and documented by Reid et al. (1995) indicate predominant rock motion in a north-north-east direction, also supporting generally southerly winds. However, some trails indicating southward motion (northerly

winds) have been seen by us, and are documented by Stanley (1955), showing that some transport occurs with northerly winds.

Until in-situ data over a significant period elucidates the micrometeorology of the playa, we suggest that (for example, for the purpose of Monte-Carlo models of rock movement) the proportion of southerly to northerly winds is between 1:1 and 10:1 and may be estimated at 4:1 (i.e. northerlies between 10% and 50% of the time, probably 20%).

4. In-Situ Measurements

As part of a NASA development program in event-triggered meteorological systems (for studying dust devils), we installed compact instrumentation for trials at the playa. One unit performed timelapse imaging to evaluate the state of the playa. The unit used an inexpensive digital camera ('Flycam One', ACME OHG, Germany), marketed for use in radio-controlled aircraft. This device records a 640x480 pixel color image to a memory card. A Picaxe-08M microcontroller (Revolution Education Ltd, UK) triggered the acquisition of an image at hourly intervals, although the camera does not record an image when it is too dark. The timelapse system was powered with a set of alkaline C-cells and was packaged in a black die-cast aluminium box 6x12x20cm and set in the cliffs at the south end of the playa. Over the observation period from 29th November 2007 to 3rd March 2008 some 1100 images were acquired. Some images were partially corrupted by a filesystem problem with low-voltage operation of the SD memory card to which the images were recorded, but the state of the playa could nonetheless be evaluated. A second camera system experienced more severe filesystem difficulties and while a few images could be recovered, they are not discussed here. Further details of the camera system, its performance and science results from dust devil observations at other sites will be discussed in a future paper.

A datalogger, using a Basic Stamp IIe microcontroller (Parallax, Inc) to record temperature and humidity (SHT-11 sensor) at 15-minute intervals, was installed in the cliffs at the south end of the playa, about 30m above the playa floor. This unit was powered by AA alkaline cells in a black plastic box 5x7x15cm. A second datalogger using a Picaxe microcontroller was installed near the eastern mid edge of the playa : although a partial temperature and pressure record was obtained, the operations of this unit were curtailed, apparently by the box becoming flooded (an ironic fate given the overall dryness of the Park!). The equipment and the study locations were approved by National Park Service personnel on a visit to the playa in May 2007 (study #DEVA-00169); the small size of the equipment means it has no visible impact on the playa. Study results are on file with the Park Service.

Most of the images of course show the same barren, empty playa. However, on three principal occasions during the study period, the playa changes drastically due to precipitation (see figure 10). These image data allow us to determine that the playa was wet for 1-2 days on three occasions during the 2007-2008 winter. Inspection of the playa in March 2008 suggests that no new trails were formed that winter, although some fading of previous trails may have occurred.

[FIGURE 10 HERE]

The temperature record (Figure 11) shows that freezing in the cliffs occurred remarkably often – some 50 times in the study period. This is remarkable given that the datalogger was in the south cliffs, and thus did not see much cold sky. On the other hand, at this location the datalogger was not exposed to direct sunlight. The minimum temperature observed was -5C, close to New Year's Eve. Such frequent freeze-thaw cycling is likely a major factor in the production of rock splinters from the cliffs which eventually reach the playa to become moving rocks. Although difficulties with a second datalogger at a more exposed location at the eastern side of the playa prevented full recovery of its data, it appears to

have experienced even colder temperatures (below -10C), as might be expected given its location in the cold air sump and with a near-unobstructed view of the sky.

The humidity record (Figure 12) in the cliffs is likely muted in terms of the total range – in the rocks the sensor likely was exposed to moister conditions than a more exposed location. Three major humidifying events (reaching 100% relative humidity for more than one sequential night) are observed, consistent with the playa imaging record, although other occasions of high humidity are seen upon which the familiar diurnal cycle oscillates.

[FIGURE 11 HERE]

[FIGURE 12 HERE]

5. Relationship of Regional Weather with Conditions on the Playa

A principal objective of the present paper is to determine whether readily-available on-line meteorological data can provide an indication of conditions at the playa. Overall weather systems in the region show reasonable correlations, and as an example we plot the RAWS humidity data over the in-situ playa humidity measurements in Figure 13. It is seen that the playa data track the regional data (itself sufficiently well-correlated that it was futile to attempt to label the curves separately), and thus the stations we have examined indeed are useful as guides for changes on daily timescales. Of course, the detailed excursions, and notably the minimum temperatures, will be highly location-dependent, even within the playa itself.

[FIGURE 13 HERE]

[FIGURE 14 HERE]

Figure 14 compares the playa wetting events determined from our imagery with the precipitation recorded at the RAWS sites. While the small size of this dataset precludes definitive statements, it suggests that winter rainfall of tens of mm recorded at the nearby RAWS stations is likely (~75%) to be associated with wetting of the playa; there is similarly a chance that a given station may not record much rain even if the playa is wetted (e.g. an event around January 29, 2008 (2008.092) affected several stations but did not flood the playa. The most accurate (or perhaps just the most 'lucky') proxy stations in the 2007-2008 season appear to be Panamint Springs, Oriental Wash and Oak Creek. Even though the Hunter Mountain site is geometrically closest to the playa, it appears to experience (see also figure 5) systematically lower precipitation than other sites due to its particular location and thus may be a less reliable indicator of playa conditions.

6. Conclusions

We have reviewed data from meteorological stations near Racetrack Playa, Death Valley National Park, and compared with a limited set of in-situ data, with a view to understanding the frequency with which necessary conditions for rock movement occur. Precipitation and evaporation data suggest the playa is wet only a few days a year, a rough guide being the number of times per year that playas in this region may be wet for N days is roughly 1/N. The number of freezing nights at Racetrack Playa may be of the order of 50 per year – rather higher than might be expected from its elevation alone. The geometry of the nearby terrain is likely responsible.

We have no data on the frequency of wind as a function of speed at the playa itself, and speed records from other sites are likely to be only of limited utility since the mountainous terrain around the

playa, and the flatness of the playa itself, are likely to be significant factors in controlling the local winds that cause rock movement. However, regionally, the winds appear to be predominantly (between 50 and 90% of the time) from the South, consistent with the majority of observed rock tracks.

Future field studies would be useful in improving the knowledge of the statistics of the relatively infrequent playa wetting events, and on the local variability of conditions around the playa itself. The most significant present gap in our knowledge is of the very localized wind speeds and directions on the playa. Together, statistics on these meteorological parameters can be applied towards stochastic models of rock formation, motion and destruction, to gain a quantitative insight into the weather-driven geological processes at this most remarkable of locations.

Acknowledgements

This work was funded in part by the NASA Applied Information Systems Research (AISR) program. BJK acknowledges a research grant from the Geological Society of America, and discretionary support from the Director of the Lunar and Planetary Laboratory, University of Arizona. We thank David Choi and Catherine Neish for assistance in the field. We are grateful for the assistance of David Ek, Wilderness Resources Coordinator at Death Valley National Park in conducting the in-situ measurements.

References

Bland, W. and D. Rolls 1998. Weathering – An Introduction to the Scientific Principles, Oxford University Press, New York, USA.

Clements, C. B, C. D. Whiteman and J. D. Hotel, 2003. Cold-Air-Pool Structure and Evolution in a Mountain Basin: Peter Sinks, Utah. Journal of Applied Meteorology, 42, 752-768.

Kirk, L. G. 1952. Trails and rocks observed on a playa in Death Valley National Monument, California. Journal of Sedimentary Petrology, 22, 173-181.

Messina, P. 1998, The Sliding Rocks of Racetrack Playa, Death Valley National Park, California: Physical and Spatial Influences on Surface Processes, Ph.D Thesis, City University of New York.

Messina, P. and P. Stoffer 2000, Terrain analysis of the Racetrack Basin and the sliding rocks of Death Valley, Geomorphology, 35, 253-265.

Reid, J. B., Bucklin, E. P., Copenagle, L., Kidder, J., Pack, S. M., Polissar, P. J., and Williams, M. L. 1995. Sliding rocks at the Racetrack, Death Valley: What makes them move? Geology, 23(9): pp. 819-822.

Roof, S. and C. Callagan, The Climate of Death Valley, California, Bulletin of the American Meteorological Society, 1725-1739, December 2003

Schumm, S. A. 1956. The movement of rocks by wind. Journal of Sedimentary Petrology, 26: pp. 284-286.

Sharp, R. P. and Carey, D. L. 1976. Sliding Stones, Racetrack Playa, California. Geological Society of America Bulletin, 87: pp. 1704-1717.

Stanley, G. M., 1955. Origin of playa stone tracks, Racetrack Playa, Inyo County, California, Geological Society of America Bulletin, 66, 1329-1350.

Figure 1. A rock (~30cm long) with trail on Racetrack Playa. Note that the trail, which obliterates earlier dessication cracks, has slightly raised edge and termination, showing the rock 'bulldozed' the playa mud when it was soft.

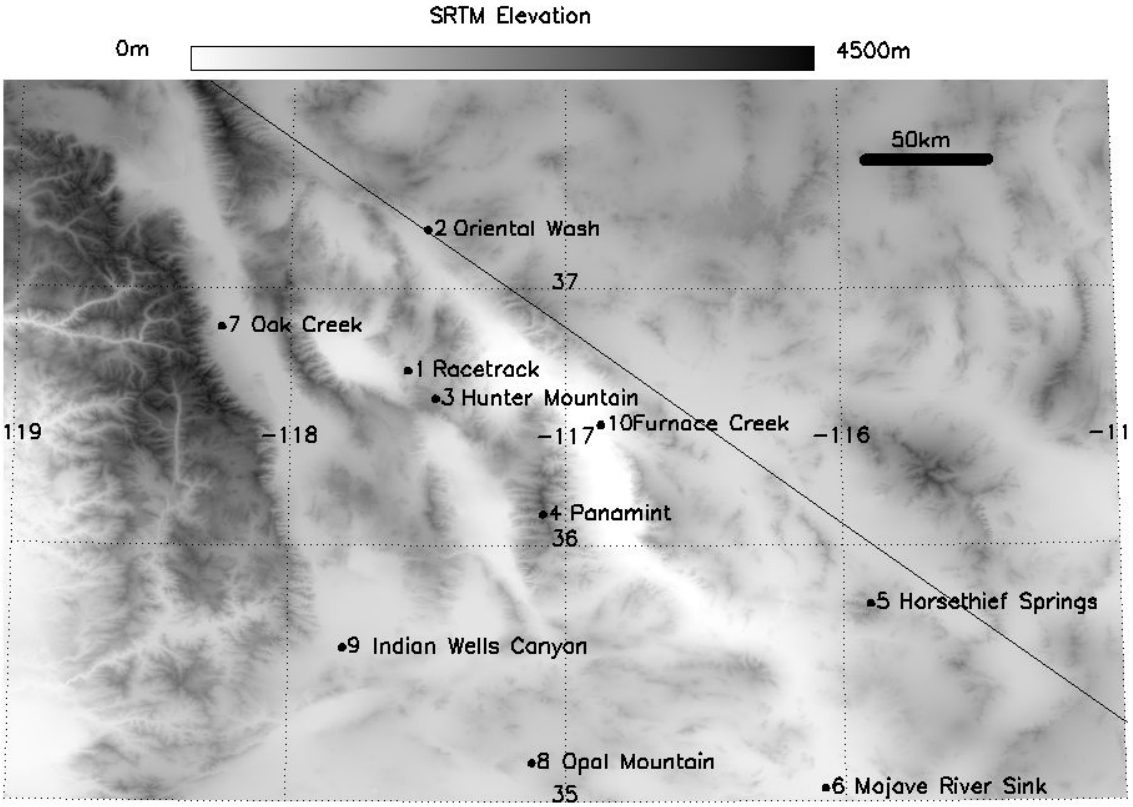

Figure 2. Regional Map of the California/Nevada border area around Death Valley National Park, showing the location of the playa (1) and the RAWS stations studied here (2-9). The map is shaded with elevation from the Shuttle Radar Topography Mission - note the serpentine white feature in the center of the map – Death Valley itself, near or in some cases below sea level.

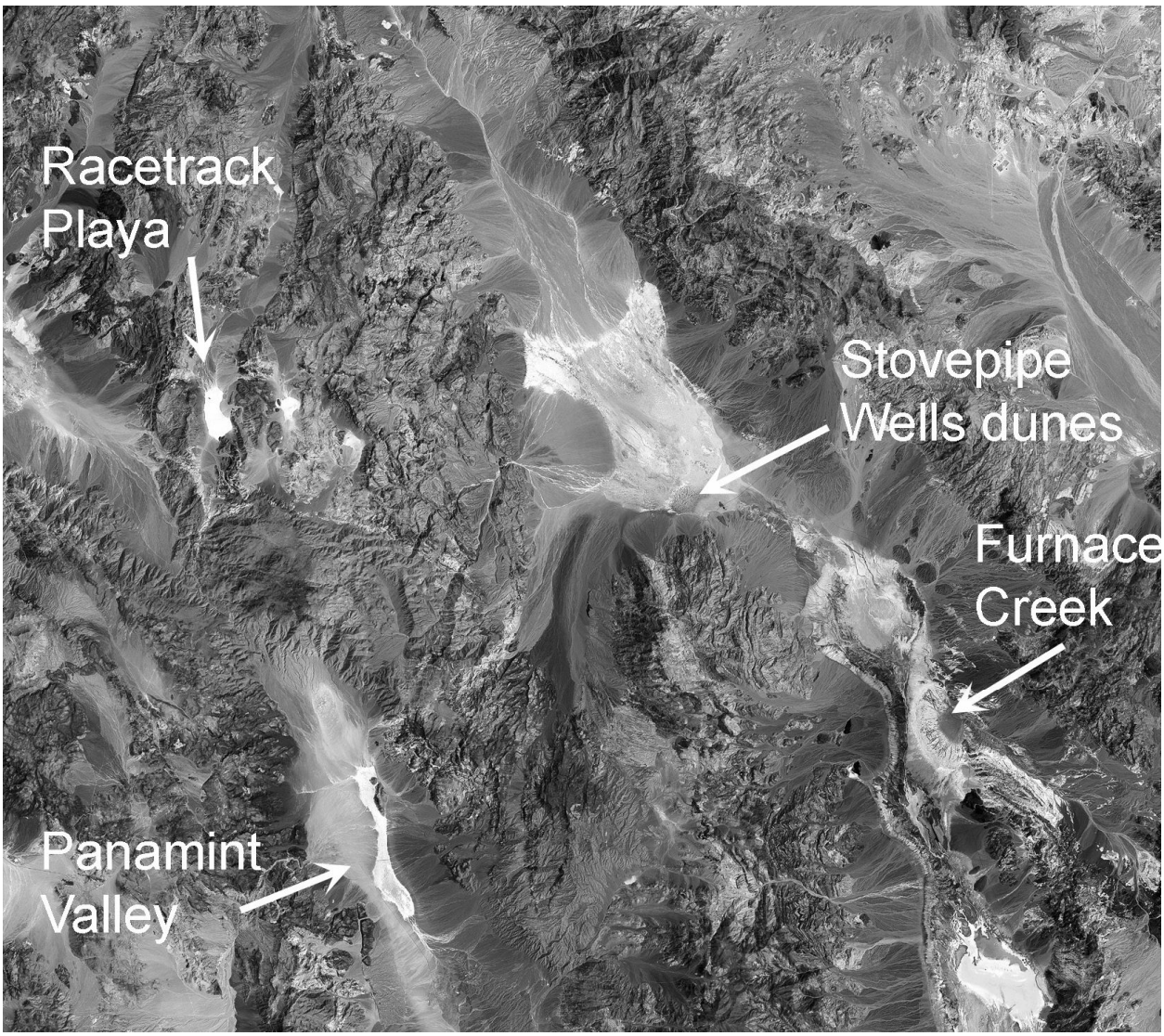

Figure 3. Landsat image showing principal locations in Death Valley National Park. The bright playa deposits at the Racetrack, at Panamint and in the main valley itself at right (Stovepipe Wells and Badwater south of Furnace Creek) are readily apparent.

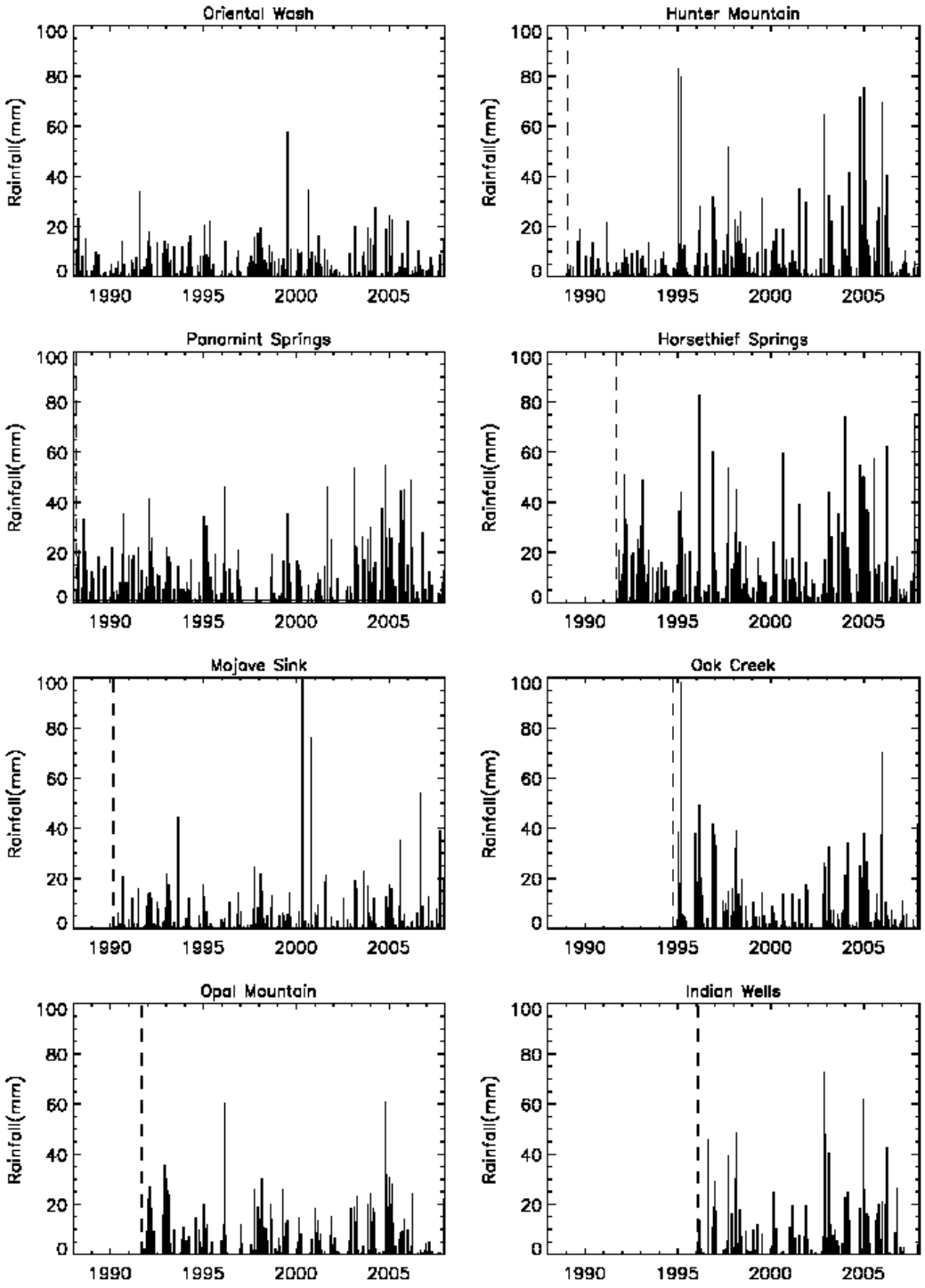
Oriental Wash
Hunter Mountain
Panamint Springs
Horsethief Springs
Mojave Sink
Oak Creek
Opal Mountain
Indian Wells
Rainfall(mm)
0
20
40
60
80
100
1990
1995
2000
2005

Figure 4. RAWS precipitation records, showing the characteristic desert pattern of infrequent, but sometimes heavy, rain. A hint of a 5-7-year periodicity can be seen in the envelope of the data. Dashed vertical line denotes the start of that station's record.

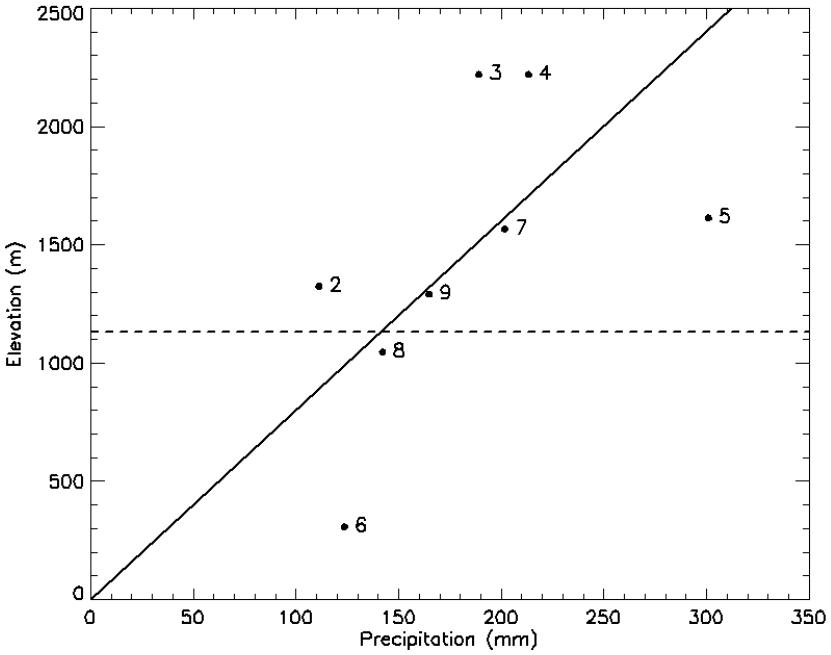

Figure 5. Annual precipitation recorded at the RAWS sites. The diagonal line (1 mm precipitation per 8m elevation rise) is merely to illustrate an easy-to-remember overall trend is not a formal fit. Dashed line shows the elevation of Racetrack Playa, suggesting an annual precipitation of 140mm is typical for the region at this elevation. Nearby Hunter Mountain (station 2) actually receives a little less, despite being higher up.

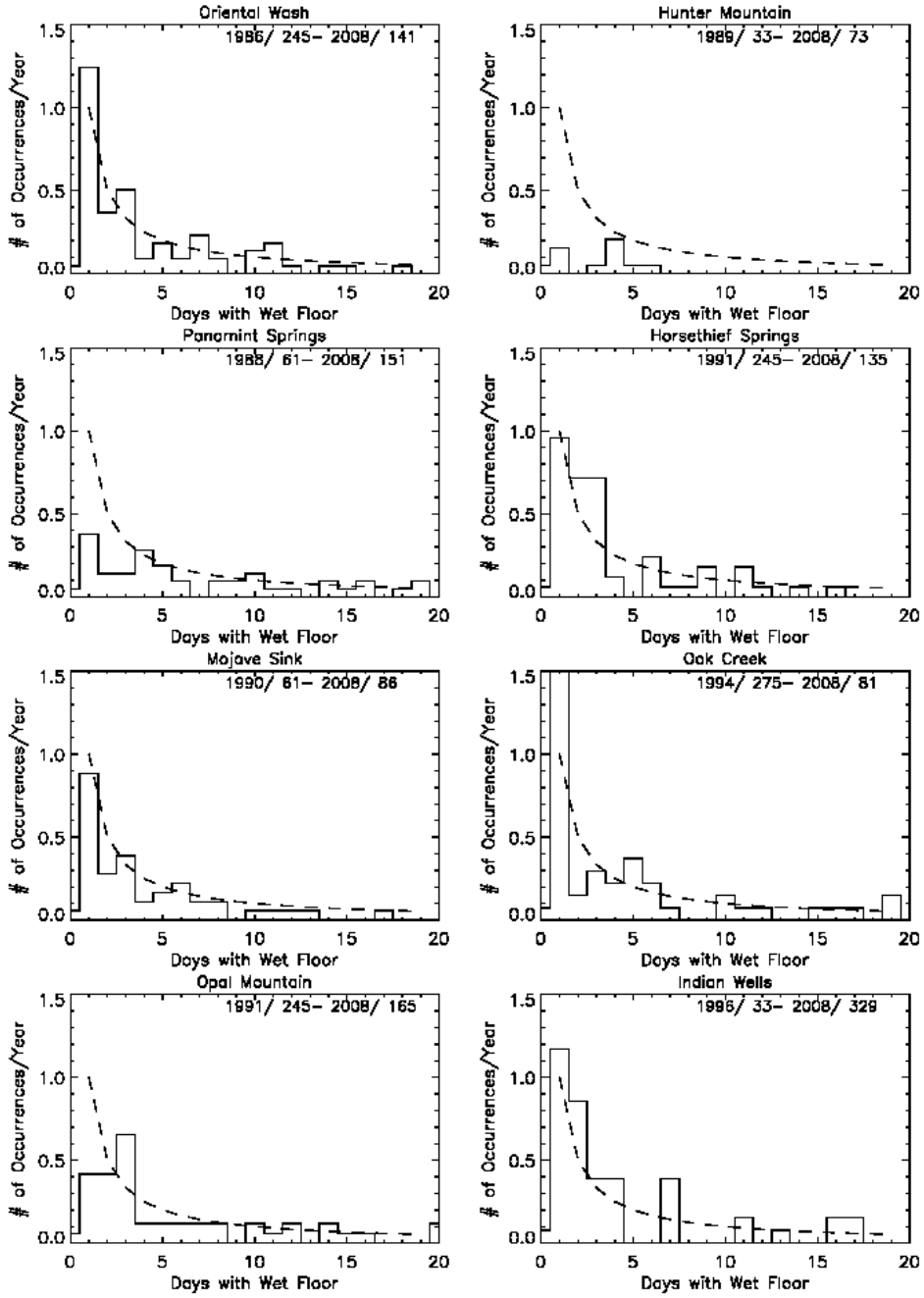

Figure 6. Frequency of episodes where the ground remains wet for some number of days is calculated by subtracting the Penman evaporation following a precipitation event. The dashed curve is a crude (1/N) fit which broadly describes the data.

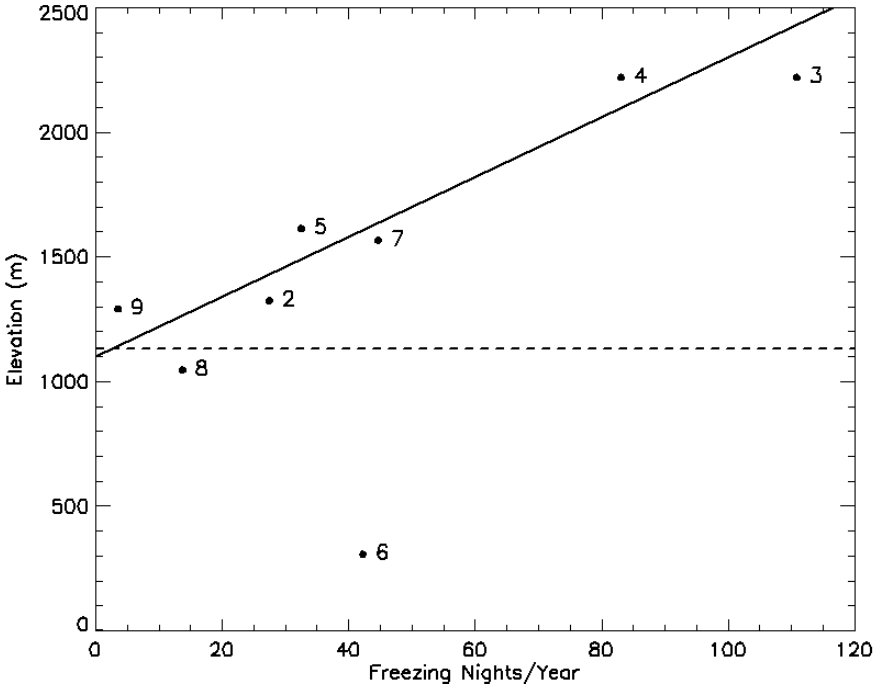

Figure 7. The number of days on which the maximum temperature exceedsthe freezing point while the minimum is below it. The outlier (6) is Mojave River Sink – see text. The line is #Nights=(Elevation-1100)/12

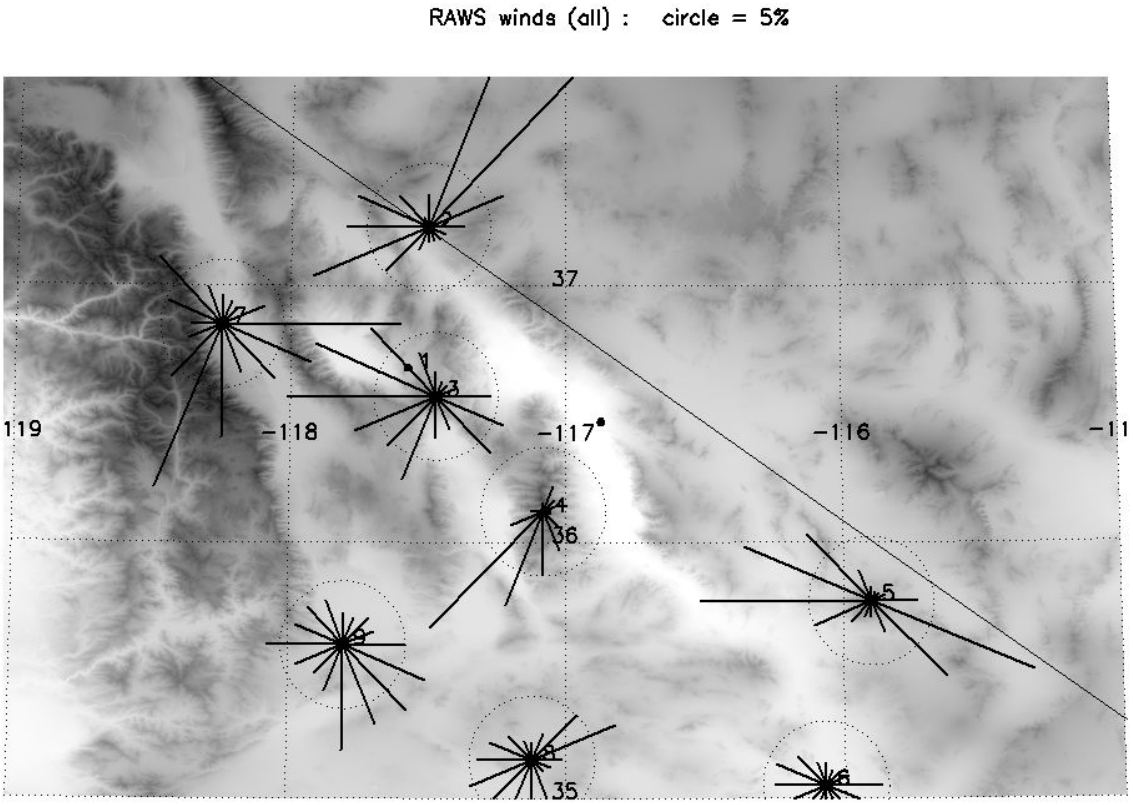

Figure 8. Conventional wind rose plots for the RAWS stations near the playa. Circles correspond to 10% of the time. The majority of winds near the playa (Stations 3,4,7,8,9) come from the South, although Oak Creek (Station 2, north of Death Valley) sees significant local north-easterly winds.

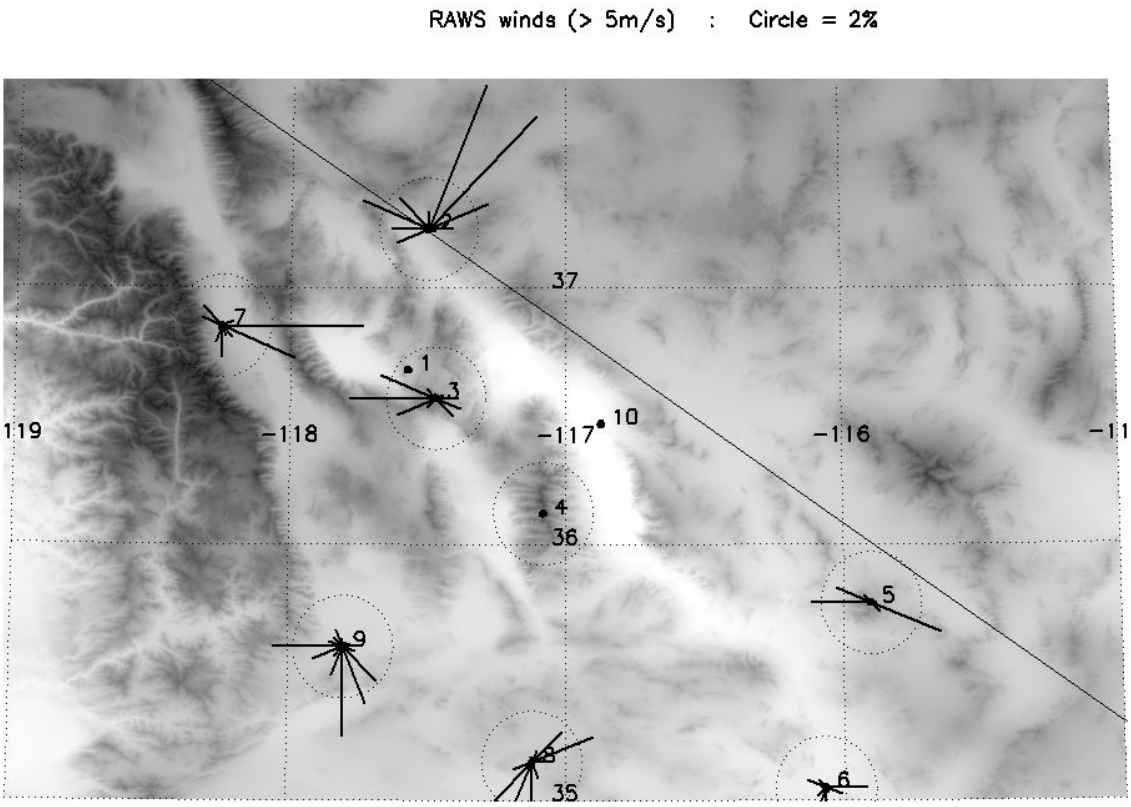

Figure 9. Modified wind roses, showing the direction of only the strongest winds retains the same pattern, with most (>75%) of the winds likely corresponding to winds that blow from south to north on the playa.

Figure 10. A sequence of images from a timelapse camera looking due north at Racetrack Playa, spanning about 40 hours circa 2007.93 (December 10-11). The dry playa is nearly featureless before a storm deposits snow in the foreground and partly floods the playa. As the snow melts, the playa floods completely, becoming a near-perfect mirror, yet within a few hours begins to dry out, showing temporary patchy dessication patterns.

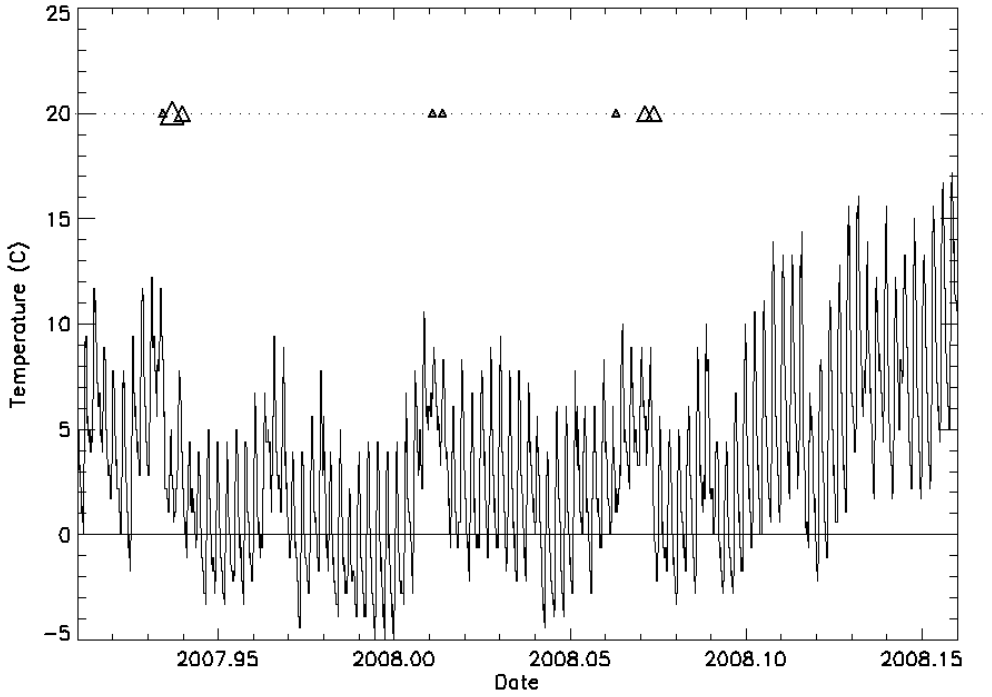

Figure 11. Temperature history in a north-facing alcove in the rocks at the south end of Racetrack Playa over December 2007-February 2008. Note that the freezing point is crossed some fifty times.The small and large triangles denotes those days when images showed partial and total playa flooding, respectively.

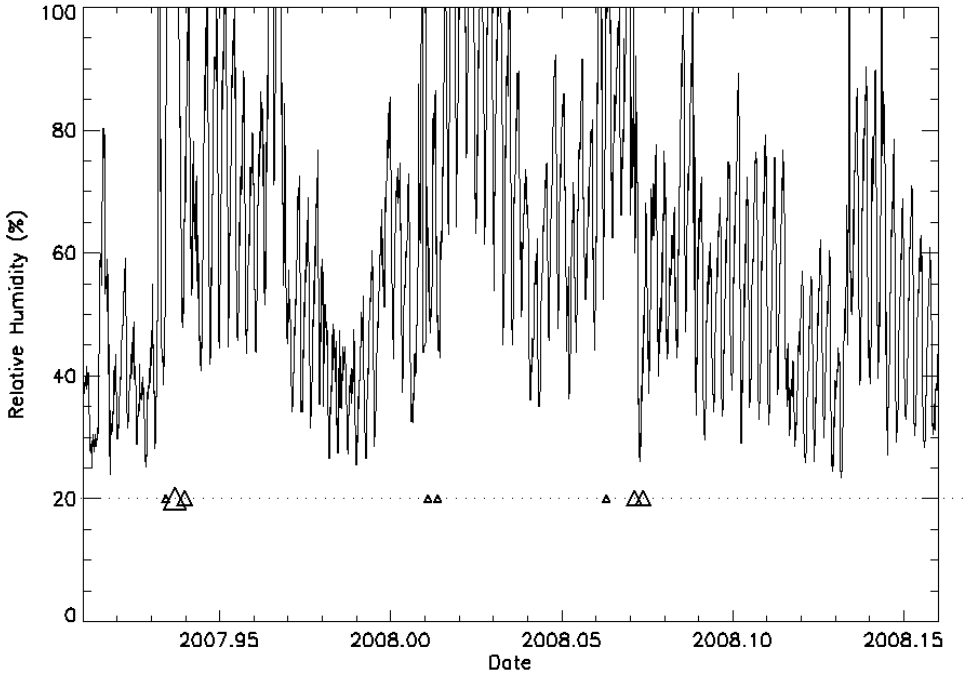

Figure 12. As for figure 11, but for relative humidity.

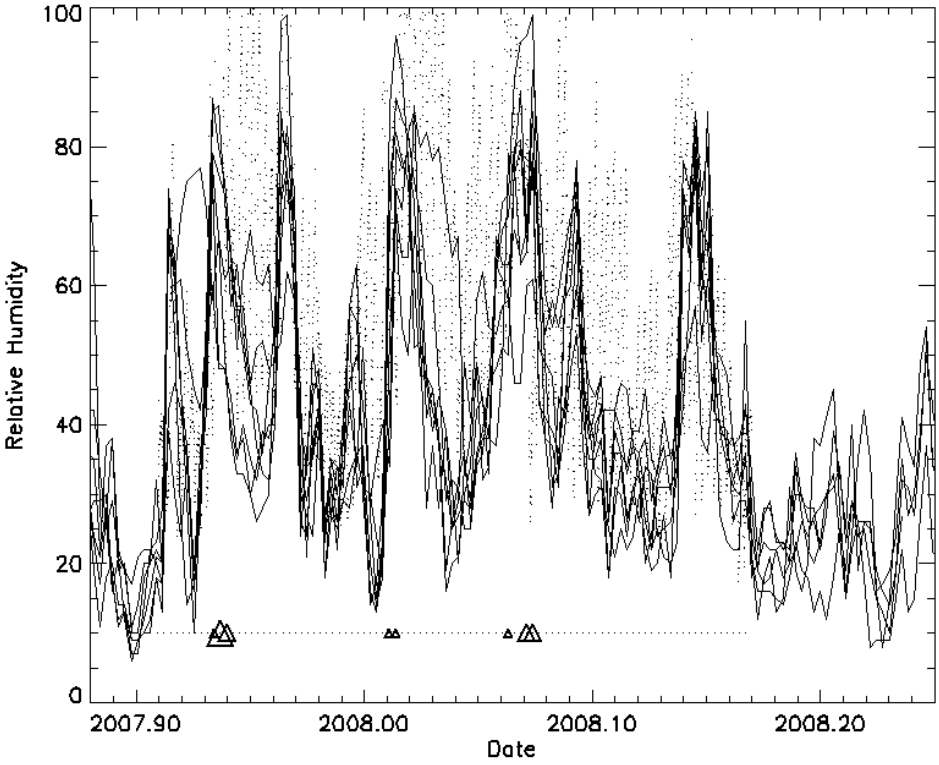

Figure 13. The RAWS humidity records for winter 2007-2008 are plotted (lines) over the humidity data recorded at the playa (points – see figure Y). The overall correlation is quite good.

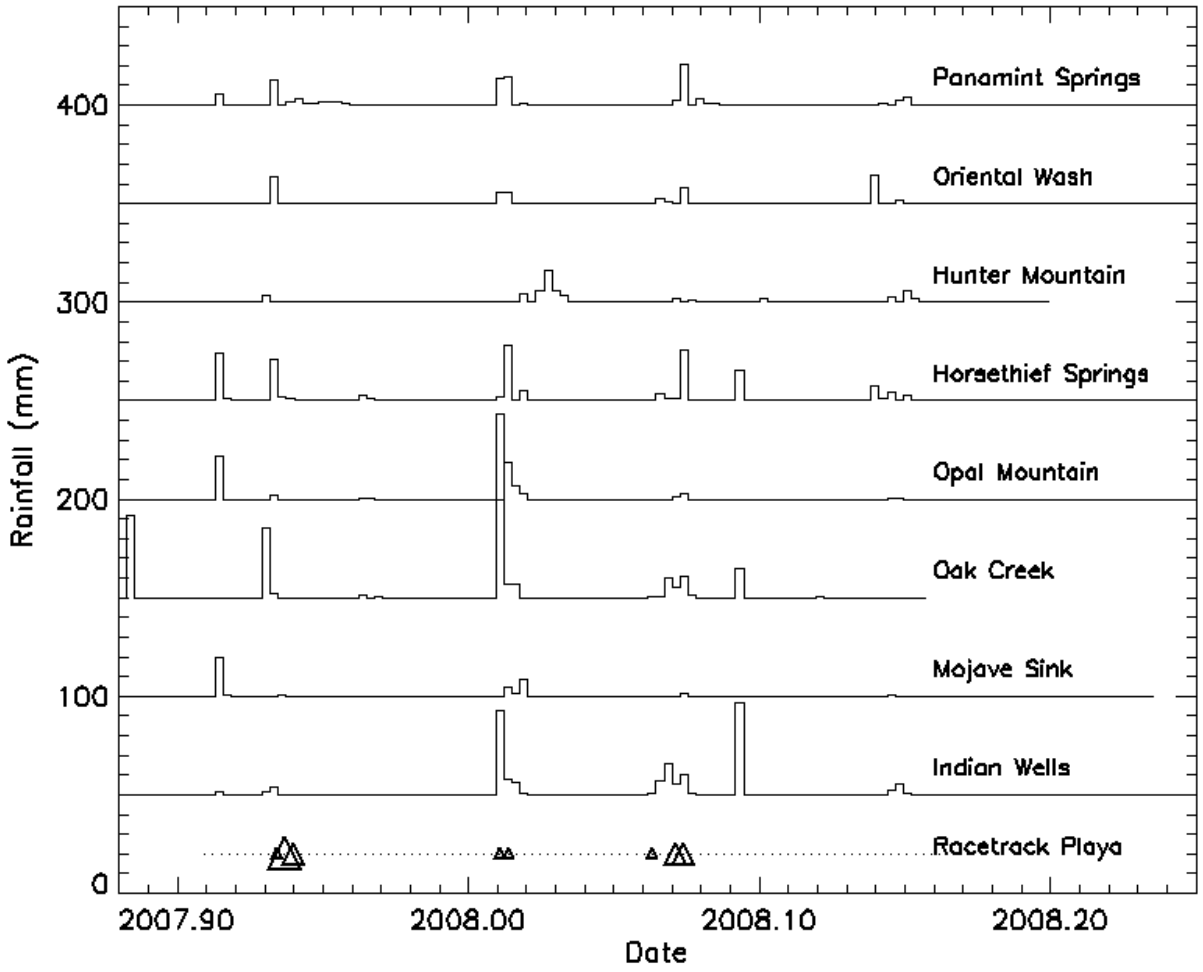

Figure 14. Rainfall records from RAWS stations over the 2007-2008 winter (successive plots offset for clarity) show events that correlate, albeit imperfectly, with occasions when Racetrack Playa was flooded.

Table 1. Location of Racetrack Playa and the RAWS stations and other sites noted in this study. The distance column indicates the straight-line distance from the playa.

#	RAWS	Site	Latitude (N)	Longitude (W)	Elevation (m)	Distance (km)
1		Racetrack	36 ° 41 '	117 ° 34 '	1130	
2	Y	Oriental Wash	37 ° 14 '	117 ° 30 '	1323	61
3	Y	Hunter Mountain	36 ° 34 '	117 ° 28 '	2219	16
4	Y	Panamint	36 ° 7 '	117 ° 5 '	2219	78
5	Y	Horsethief Springs	35 ° 46 '	115 ° 54 '	1613	189
6	Y	Mojave River Sink	35 ° 3 '	116 ° 4 '	306	231
7	Y	Oak Creek	36 ° 51 '	118 ° 15 '	1566	68
8	Y	Opal Mountain	35 ° 9 '	117 ° 7 '	1045	176
9	Y	Indian Wells Canyon	35 ° 41 '	117 ° 53 '	1290	115
10		Furnace Creek	36 ° 28 '	116 ° 52 '	-61	71
11		Stovepipe Wells	36 ° 36 '	117 ° 8 '	8	42
12		Wildrose	36 ° 16 '	116 ° 52 '	1355	81